Optimal Mitigation Policies in a Pandemic: Social Distancing and Working from Home*

Callum Jones† Thomas Philippon‡ Venky Venkateswaran§

February 2021

Abstract

We study the response of an economy to an unexpected epidemic. The spread of the disease can be mitigated by reducing consumption and hours worked in the office. Working from home is subject to learning-by-doing. Private agents' rational incentives are relatively weak and fatalistic. The planner recognizes the infection and congestion externalities and implements front-loaded mitigation policies. In our calibrated model, private mitigation reduces the cumulative death rate by about 31% compared to more than 85% for the planner, albeit at the cost of a sharper drop in consumption. Our model can replicate industry/occupation level data on incidence rates, explain on how small differences in initial conditions can lead to large differences in outcomes across regions, and predict how on how the anticipation of a future vaccine shapes the joint dynamics of consumption and infections.

Keywords: contagion, containment, covid 19, recession, R_0, social distancing, SIR model, learning-by-doing, mitigation, suppression, vaccine.

1 Introduction

The response to the Covid-19 crisis highlights the tension between health and economic outcomes. We propose a simple extension of the neoclassical model to quantify the trade-offs and guide policy.

*We are grateful to the editor Ralph Koijen and two anonymous referees for valuable feedback. We are indebted to Fernando Alvarez, Robert Shimer, and seminar participants at the Federal Reserve Board, the University of Chicago, and the NBER Summer Institute for comments. The views expressed are those of the authors and not necessarily those of the Federal Reserve Board or the Federal Reserve System. First version: March 31, 2020.

†Federal Reserve Board, callum.j.jones@frb.gov

‡New York University, CEPR and NBER, tphilipp@stern.nyu.edu

§New York University, NBER, vvenkate@stern.nyu.edu

We are particularly interested in understanding the nature and timing of policy responses as well as the tensions between private and public incentives. When will the private sector engineer the right response in terms of timing and magnitudes? When is there a need for policy intervention?

Our model has two building blocks: one for the dynamics of contagion, and one for consumption and production, including mitigation strategies (such as working from home). Our starting point is the standard SIR model of contagion used by public health specialists. Atkeson (2020b) provides a good summary of this framework. In a population of initial size N, the epidemiological state is given by the numbers of Susceptible (S), Infected (I), and Recovered (R) people. By definition, the cumulative number of deaths is $D = N - S - I - R$. Infected people transmit the virus to susceptible people at a rate that depends on the nature of the virus and on the frequency of economic and social interactions. Mitigation efforts in the form of lockdowns and work-from-home reduce interactions and curtail the spread of the disease. The rates of recovery (transitions from I to R), morbidity (I becoming severely or critically sick) and mortality (from I to D) depend on the nature of the virus and on the quality of health care services. The quality of health services depends in turn on the capacity of health care providers (number of ICU beds, ventilators) and the number of sick people.

The economic side of the model focuses on three key decisions: consumption, labor supply, and working from home. We use a canonical macroeconomic framework with a representative household. Both consumption and work increase the risk of contagion, which is the key link between the economic and epidemiological blocks of the model. We endow agents with the option to undertake exposure-mitigating actions (e.g. working from home) that reduce contagion risk but lower productivity. Productivity losses decline as agents accumulate experience in working from home. This learning-by-doing aspect introduces additional dynamic considerations in the household's problem.

We use a calibrated version of the model to study the reaction of private agents and a social planner to the announcement of an outbreak. Upon learning of the risks posed by the virus, households cut spending and labor supply and increase time spent working from home. Their mitigation efforts are approximately proportionate to the risk of infection, which – all else equal – is proportional to the fraction of infected agents I/N. The planner's response differs from the response of private agents because of two externalities. The first is the usual infection externality: households only take into account the risk that they become infected, not the risk that they infect

others. The other is is a congestion externality in healthcare: agents do not internalize the fact that the treatment they receive if they become sick reduces the amount of healthcare services available for other agents. Both these factors make private mitigation lower than the socially optimal level. We show that this wedge between private and social incentives can be particularly severe early on in the outbreak. When private agents become aware of the disease, the possibility of future infection reduces the value of being careful today. We term this the fatalism effect. The planner, on the other hand, internalizes the possibility of infecting others and a congested healthcare system and, as a result, her incentives to avoid infection increase sharply when she learns of the disease.

Our quantitative results show that this wedge has significant implications for the evolution of both macro and health outcomes. In equilibrium, the representative household's private response closely tracks the path of the infection rate. At the peak, labor supply drops by about 7%, while 27% of workers work from home. The result is a time-path for infections that peaks at the same time as the zero-mitigation time-path, albeit at a lower level. The decentralized equilibrium features significant congestion in healthcare at the peak of the epidemic when the fatality rate is just over double the baseline level. The ultimate cumulative deaths is over 0.33% of the population. The planner, on the other hand, acts more quickly and aggressively to flatten the curve – both by cutting labor supply by a bit more (12%) as well as prescribing stronger mitigation (work-from-home ratio of 50% at the height). The infection rate peaks a few weeks later and at a much lower level than that of the equilibrium level. The peak fatality rate and the cumulative fatalities are also significantly reduced. The ability to mitigate by working from home plays a significant role in ameliorating the economic impact of the mitigation strategies. While this is true in both cases, the planner uses this option much more intensively than private agents would. Without the option to work from home, the planner's optimal strategy would have a peak drop in consumption of almost 25% (compared to 15% in the baseline model). Working from home is therefore a critical element of the public response to the epidemic.

The quantitative predictions of the model are consistent with the outcomes observed in the state of New York. From March to September 2020, GDP in New York fell by 10.5% relative to trend while cumulative excess deaths were 0.21% of the population. Under the optimal solution in our model, over the first 26 weeks, the average decline in GDP from the pre-pandemic state is 12% while about 0.17% of the initial population die from the disease.

We then use disaggregated sector-level data to further test the predictions of the model. We first extend our model by considering multiple sectors which differ in their exposure risks and the cost of working from home. We find that the optimal path of mitigation matches well the cross-sectoral patterns in both epidemiological and economic outcomes. By week 26 after the outbreak of the pandemic, the sectors with the highest exposure risk account for 64% of cumulative infections and have a decline in GDP of about 10%. This prediction is consistent with data from Washington state where, in 2020 Q2 and Q3, the high infection sector accounts for 65% of cumulative infections and had a decline in GDP of 8%.

We then examine the robustness of our main results to assumptions about parameters (notably the fatality rate) and the arrival of news about the disease. We explore the planner's incentives to mitigate under time-varying parameters and when we explicitly model fatigue associated with mitigation efforts. We also consider a version of the model with altruistic households and find that a high degree of altruism is necessary to get close to the planner's outcomes. Finally, we use the model to guide decision-making under uncertainty about key epidemiological parameters (the reproduction number and the fatality rate). The analysis reveals that, despite this uncertainty, the planner can get quite close to her optimal strategy by actively suppressing the disease in its early stages while waiting for incoming data to resolve the uncertainty. Intuitively, this is possible because her optimal strategy in the first few weeks remains quite similar across a wide range of fatality and infection parameters.

Literature There are a number of papers studying the trade-off between economic and health outcomes in the context of the Covid-19 pandemic. It is impossible to cite every paper from this large body of work, so we restrict ourselves to the most closely related early ones – Barro et al. (2020), Eichenbaum et al. (2020) and Alvarez et al. (2020). Barro et al. (2020) and Correia et al. (2020) draw lessons from the 1918 flu epidemic. Barro et al. (2020) find a high death rate (about 40 million people, 2% of the population at the time) and a large but not extreme impact on the economy (cumulative loss in GDP per capita of 6% over 3 years). The impact on the stock market was small. Correia et al. (2020) find that early interventions help protect health and economic outcomes. Our paper also relates to an older literature on contagion dynamics, e.g. (Diekmann and Heesterbeek, 2000). We refer to the reader to Atkeson (2020b) for a recent discussion. Berger

et al. (2020) show that testing can reduce the economic cost of mitigation policies as well as reduce the congestion in the health care system. Baker et al. (2020) document the early consumption response of households in the US.

Our model shares with Eichenbaum et al. (2020) the idea of embedding SIR dynamics in a simple macroeconomic framework. The SIR block is the same, but there are some notable differences in the economic model. Eichenbaum et al. (2020) consider hand-to-mouth agents who know their health status, while we use a representative household framework in the tradition of Lucas and Stokey (1987), where both consumption and health risks are pooled, and asymptomatic agents are unaware of their status. We also allow for a distinct margin of mitigation, interpreted as work-from-home, along with a learning-by-doing structure, which adds an important dynamic element. By mitigating today, the planner invests in the new technology to mitigate future disruptions. We also highlight the dynamic tension (the so-called fatalism bias) between the planner and the private sector's incentives.

2 Benchmark Model

2.1 Households

There is a continuum of mass N of households, and time is measured in weeks. Each household is of size 1 and the utility of the household is

$$U = \sum_{t=0}^{\infty} \beta^t u\left(c_t, l_t; i_t, d_t\right),$$

where c_t and l_t are per-capita consumption and labor supply. The household starts with a continuum of mass 1 of family members, all of them susceptible to the disease. At any time $t > 0$, we denote by s_t, i_t and d_t the numbers of susceptible, infected and dead people. The size of the household at time t is therefore $1 - d_t$, and total household consumption is $(1 - d_t)\, c_t$. Among the i_t infected members, κi_t are too sick to work. The labor force at time t is therefore $1 - d_t - \kappa i_t$, and household labor supply is $(1 - d_t - \kappa i_t)\, l_t$. The number of household members who have recovered from the

disease is $r_t = 1 - s_t - i_t - d_t$. In our quantitative analysis, we use the functional form

$$u\left(c_t, l_t; i_t, d_t\right) = \left(1 - d_t - \kappa i_t\right)\left(\log\left(c_t\right) - \frac{l_t^{1+\eta}}{1+\eta}\right) + \kappa i_t\left(\log\left(c_t\right) - u_\kappa\right) - u_d d_t, \tag{1}$$

where u_κ is the disutility from being sick and u_d the disutility from death which includes lost utility and the psychological cost on surviving members. For simplicity, we assume that sickness does not change the marginal utility from consumption. This implies that the household will equate consumption for all alive members (i.e. independent of health status). The variables s_t, i_t and d_t evolve according to a standard SIR model described below.

At the beginning of time t, each household decides how much to consume c_t (per capita) and how much each able-bodied member should work l_t. We have normalized the disutility of labor so that $l = c = 1$ before the epidemic starts. Households become infected by shopping and by going to work. We compute infection in two steps. First, we define exposure levels for shoppers and for workers. Then, we aggregate these into a composite infection rate at the household level. We assume throughout the paper that asymptomatic individuals are unaware of their infection. Formally, $\{dead\}$ and $\{sick\}$ are the only observable states at the individual level. In particular, households cannot tell the difference between the s_t members who are susceptible and the $(1-\kappa)\, i_t$ members who are infected but not sick. This modeling choice is the main difference between our model and the model of Eichenbaum et al. (2020) who make the polar opposite assumption. They assume that individuals know their types, do not share risks within a family, and behave in a hand-to-mouth fashion. We follow instead a Lucas and Stokey (1987) approach to model households' decisions and risk sharing, so our model stays close to a standard representative agent model.

2.2 Exposure from Consumption

Consumption exposure is given by

$$e^c c_t C_t, \tag{2}$$

where e^c is a parameter which indexes the sensitivity of infection risk to consumption and C_t is aggregate consumption.[1] The idea behind this specification is that household members engage in various activities related to consumption – such as shopping in a crowded mall, eating inside

[1] We use lower-case letters to denote household level variables and upper-case for aggregates.

a restaurant, going to a hospital – which exposes them to infection risk. These are assumed to be proportional to consumption expenditure c_t and for a given level of aggregate consumption, exposure is proportional to such activities.[2]

2.3 Production and Working from Home

Production uses only labor, but a key feature of our model is the distinction between hours supplied by able bodied workers l_t and effective labor supply $\hat{l}_t$ per household. Effective labor supply is

$$\hat{l}_t = (1 - d_t - \kappa i_t)\left(l_t - \frac{\chi_t}{2} m_t^2\right). \tag{3}$$

The first term captures the fact that the number of valid household member is decreased by death and sickness. The second term captures the cost of implementing mitigation strategies, denoted m_t (e.g., working from home at least some of the time). These strategies come at a cost – in the form of lost productivity, captured by the term $\frac{\chi_t}{2} m_t^2$. The loss process χ_t is a decreasing function of the accumulated experience working from home and is given by:

$$\chi_t = \chi\left(\overline{m}_t\right),$$

where $\overline{m}_t$ is the stock of accumulated mitigation (with a depreciation rate of $1 - \rho_m$)

$$\overline{m}_{t+1} = \rho_m \overline{m}_t + m_t. \tag{4}$$

The function χ is positive, decreasing, and convex. We assume the following functional form

$$\chi_t = \bar{\chi}\left(1 - \Delta_\chi\left(1 - \exp\left(-\overline{m}_t\right)\right)\right). \tag{5}$$

The cost shifter initially (i.e. when $\overline{m}_t$=0) is equal to $\bar{\chi} > 0$ and then falls over time as people figure out how to work from home. The parameter $\Delta_\chi$indexes the maximum potential for learning by doing, since as $\overline{m}_t$ becomes large, the cost approaches $\bar{\chi}\left(1 - \Delta_\chi\right)$. The benefit of mitigation

[2]Our baseline model is a simple one-sector economy. In our quantitative analysis, however, we will explore an extension with multiple sectors which differ in their exposure risks and mitigation possibilities.

strategies is a reduction in the risk of infection. Specifically, exposure from work is given by

$$e^l (1 - m_t) l_t (1 - M_t) L_t,$$

where, as before, upper-case letters denote aggregates. The aggregate resource constraint is

$$Y_t = C_t = \hat{L}_t = N\hat{l}_t.$$

In our basic model, we ignore the issue of firm heterogeneity and market power. Therefore, price is equal to marginal cost

$$P_t = W_t = 1,$$

where W_t is the wage per unit of effective labor, which we normalize to one.

2.4 Income and Contagion

At the end of each period, household members regroup and share income and consumption. Household labor income is $W_t\hat{l}_t = \hat{l}_t$ and the budget constraint is

$$(1 - d_t) c_t + \frac{b_{t+1}}{1 + r_t} \leq b_t + \hat{l}_t. \tag{6}$$

Total exposure for the household is defined as

$$e_t = \bar{e} + (1 - d_t) e^c c_t C_t + (1 - d_t - \kappa i_t) e^l (1 - m_t) l_t (1 - M_t) L_t, \tag{7}$$

where $\bar{e}$ is baseline exposure, independent of market activities. The number of susceptible, infected, dead and recovered members in a household follows a standard $SIRD$ model (see Appendix):

$$s_{t+1} = s_t - \gamma e_t \frac{I_t}{N} s_t \tag{8}$$

$$i_{t+1} = \gamma e_t \frac{I_t}{N} s_t + (1 - \rho) i_t - \delta_t \kappa i_t \tag{9}$$

$$d_{t+1} = d_t + \delta_t \kappa i_t \tag{10}$$

$$r_{t+1} = r_t + \rho i_t, \tag{11}$$

where γ is the infection rate per unit of exposure, ρ the recovery rate, κ the probability of being sick conditional on infection, and δ_t the mortality rate of sick patients. Recall that exposure e_t depends on consumption, labor supply and mitigation strategies, as characterized in 7. Note that the number of new infected, $\gamma e_t \frac{I_t}{N} s_t$, is a function of the aggregate infection rate, $\frac{I_t}{N}$, taken as given by individual households. Finally, the mortality rate δ_t is described by an increasing function of the measure of sick agents:

$$\delta_t = \delta\left(\kappa I_t\right),$$

which captures the idea that an overloaded healthcare system can contribute to higher fatalities.

Finally, in this framework, a simple way to model a vaccine is by varying the exposure parameter γ. If a fraction v of the susceptible population has been inoculated with a fully effective vaccine, the effective γ in (8)-(9) is $\gamma\left(1-v\right)$. This is the approach we will take in our quantitative analysis – for now, we abstract from this and treat γ as a constant.

2.5 Market Clearing and Aggregate Dynamics

Infection dynamics for the the entire population are simply given by the SIR system above with aggregate variable $I_t = N i_t$, and so on. The aggregate labor force and total consumption are equal to $N\left(1-\kappa i_t - d_t\right) l_t$ and $N\left(1-d_t\right) c_t$ respectively. The market clearing conditions for goods and bonds are given by

$$\begin{aligned}\left(1-d_t\right) c_t &= \hat{l}_t \\ b_t &= 0.\end{aligned}$$

3 Decentralized equilibrium

3.1 Equilibrium Conditions

Since our model reduces to a representative household model and since $b = 0$ in equilibrium, we simply omit b from the value function. The household's optimal choices are the solution to the following recursive problem:

$$V\left(i_t, s_t, d_t, \overline{m}_t\right) = \max_{c_t, l_t, m_t} u\left(c_t, l_t; i_t, d_t\right) + \beta V\left(i_{t+1}, d_{t+1}, s_{t+1}, \overline{m}_{t+1}\right),$$

where the period utility function is defined in (1). The full set of optimality conditions for this problem are given in the Appendix. In what follows, we let $\{\lambda_t, \lambda_{e,t}, \lambda_{i,t}, \lambda_{s,t}, \lambda_{d,t}\}$ denote the Lagrange multipliers with respect to the budget constraint (6), the exposure equation (7), and the three independent SIR equations (8) to (10). We denote by $\{V_{i,t}, V_{s,t}, V_{d,t}, V_{\bar{m},t}\}$ the envelope conditions with respect to the state variables.

The first order conditions for consumption and labor are

$$\begin{aligned} c_t^{-1} &= \lambda_t + \lambda_{e,t} e^c C_t \\ l_t^{\eta} &= \lambda_t - \lambda_{e,t} e^l \left(1 - m_t\right)\left(1 - M_t\right) L_t. \end{aligned}$$

These two expressions show how consumption and labor fall with higher exposure risk, summarized by $\lambda_{e,t}$, the Lagrange multiplier on the exposure equation. The first order condition with respect to work-from-home mitigation is

$$\lambda_t \chi_t m_t = \frac{\beta V_{\bar{m},t+1}}{1 - d_t - \kappa i_t} + \lambda_{e,t} e^l l_t \left(1 - M_t\right) L_t,$$

so that mitigation efforts rise with exposure risk.

3.2 Equilibrium with Exogenous Infections

To simplify the notation, we normalize $N = 1$, so we should think of our values as being per-capita pre-infection. When there is no risk of contagion, i.e. $i_t = 0$, $\lambda_{e,t} = 0$ and $V_{\bar{m},t+1} = 0$, we have $m_t = 0$ and from the optimal consumption and labor supply

$$c_t^{-1} = l_t^{\eta}.$$

Since $m = 0$, we have $\hat{l}_t = l_t$, so market clearing is simply

$$c_t = l_t.$$

Combining these two conditions, we get

$$c_t = l_t = 1.$$

Thus, the pre-infection economy is always in steady state. Consider now an economy with exogenous SIR dynamics: $e^c = e^l = 0$. This implies $m_t = 0$ and

$$c_t^{-1} = l_t^{\eta}.$$

Market clearing requires

$$(1 - d_t)\, c_t = (1 - d_t - \kappa i_t)\, l_t,$$

therefore

$$l_t^{1+\eta} = 1 + \frac{\kappa i_t}{1 - d_t - \kappa i_t}.$$

The labor supply of valid workers increases to compensate for the reduced productivity of the sick. Per capita consumption is

$$c_t = \left(\frac{1 - d_t}{1 - d_t - \kappa i_t} \right)^{-\frac{\eta}{1+\eta}}.$$

As long as $\eta > 0$, consumption per capita decreases. Intuitively, aggregate GDP decreases because of lost labor productivity and deaths.

The SIR system is independent from the economic equilibrium. As described in the Appendix, the share of infected agents I_t increases, reaches a maximum and converges to 0 in the long run. Assuming a constant δ, the long run solution solves

$$\log\left(\frac{S_\infty}{1 - I_0} \right) = -\frac{\gamma \bar{e}}{\rho + \delta\kappa} \left(\frac{1 - S_\infty}{N} \right),$$

and

$$D_\infty = \frac{\delta\kappa}{\delta\kappa + \rho} \left(1 - S_\infty\right).$$

When the congestion externality arises and δ_t increases, then we cannot obtain a closed-form solution for the long run death rate but the qualitative results are unchanged. The following proposition summarizes our results.

Proposition 1. *When contagion does not depend on economic activity* $\left(e^c = e^l = 0\right)$*, the share of infected agents* I_t *increases, reaches a maximum and converges to* 0 *in the long run. The long run death rate is given by* $D_\infty = \frac{\delta\kappa}{\delta\kappa+\rho}\left(1 - S_\infty\right)$ *where the long run share of uninfected agents solves* $\log\left(\frac{S_\infty}{1-I_0}\right) = -\frac{\gamma\bar{e}}{\rho+\delta\kappa}\left(\frac{1-S_\infty}{N}\right)$*. Along the transition path, labor supply of able-bodied workers follows the infection rate while per-capita consumption moves in the opposite direction as* $c_t = \left(1 - \frac{\kappa i_t}{1-d_t}\right)^{\frac{\eta}{1+\eta}}$.

3.3 Private Incentives for Mitigation

In this subsection, we return to the model with endogenous exposure and characterize incentives of households in a laissez-faire equilibrium to undertake mitigation. These incentives depend on the shadow value of exposure $\lambda_{e,t} = \left(\lambda_{i,t} - \lambda_{s,t}\right)\gamma\frac{I_t}{N}s_t$ which is increasing in new infections, $\gamma\frac{I_t}{N}s_t$. In other words, for a given $\lambda_{i,t} - \lambda_{s,t}$, the private incentives to mitigate are proportional to the number of new cases. Now,

$$\lambda_{i,t} - \lambda_{s,t} = \beta\left(V_{s,t+1} - V_{i,t+1}\right),$$

with

$$V_{s,t} - V_{i,t} = u_\kappa\kappa + \kappa l_t\left(\lambda_t - \frac{l_t^\eta}{1+\eta}\right) - \rho\lambda_{i,t} + \left(1 - \gamma e_t\frac{I_t}{N}\right)\beta\left(V_{s,t+1} - V_{i,t+1}\right) + \delta_t\kappa\beta\left(V_{i,t+1} - V_{d,t+1}\right).$$

Fatalism Effect We now use an approximation to obtain a sharper characterization and gain more intuition. Specifically, we make the following assumptions (i) the non-monetary cost of death u_d is sufficiently large that it dominates the other terms in the expressions for $V_{d,t}$ and $V_{i,t}$ (ii) there are no congestion effects on fatality, i.e. $\delta_t = \delta$. Then, the value of death and infection are approximately constant, i.e.

$$\begin{aligned} V_{d,t} &\approx -\frac{u_d}{1-\beta} \\ V_{i,t} &\approx \sum_{s=0}^{\infty}\beta^s\left(1-\rho-\delta\kappa\right)^s\kappa\left(-u_\kappa + \delta\frac{\beta u_d}{1-\beta}\right) = \frac{\kappa u_\kappa + \delta\kappa\frac{\beta}{1-\beta}u_d}{1-\beta\left(1-\rho-\delta\kappa\right)} \equiv V_i. \end{aligned}$$

The value of avoiding an infection at time t is the discounted value of the disutility from sickness and death. The value of remaining susceptible is then

$$V_{s,t} \approx V_i \sum_{s=1}^{\infty} \beta^s \left(1 - \gamma e_{t+s-1} \frac{I_{t+s-1}}{N}\right)^{s-1} \gamma e_{t+s-1} \frac{I_{t+s-1}}{N}.$$

Importantly, $V_{s,t}$ falls with the risk of infection in the near future. Formally, we can show that

$$\frac{\partial V_{s,t}}{\partial \frac{I_{t+s-1}}{N}} = V_i \beta^s \left(1 - \gamma e_{t+s-1} \frac{I_{t+s-1}}{N}\right)^{s-1} \gamma e_{t+s-1} \left[1 - (s-1) \frac{\gamma e_{t+s-1} \frac{I_{t+s-1}}{N}}{1 - \gamma e_{t+s-1} \frac{I_{t+s-1}}{N}}\right].$$

The term inside the square bracket is positive (or equivalently, $\frac{\partial V_{s,t}}{\partial \frac{I_{t+s-1}}{N}}$ is negative) for low s. Since $V_{i,t}$ is approximately constant, this means that the difference $V_{s,t} - V_{i,t}$ *shrinks* when agents become aware of the disease, i.e. there is a perverse effect on incentives to mitigate. We term this channel *the fatalism effect*: early on, agents (correctly) anticipate that they are likely to become infected and so have weak incentives to avoid infection today. Notice, however, that this fatalism is perfectly rational and does not represent any behavioral mistake by the agents. As we will see, the planner's solution considers other forces that offset this channel. When δ is constant, the fatalism effect rationally reduces private incentives to mitigate the disease, i.e., $V_{s,t} - V_{i,t}$ is small, but it does not switch the sign, i.e., $V_{s,t} - V_{i,t}$ remains positive. This can change when δ is time varying as we discuss later.

4 Planner's Problem

Again, we normalize $N = 1$ for simplicity. The planner solves

$$\max U = \sum_{t=0}^{\infty} \beta^t u\left(C_t, L_t; I_t, D_t\right),$$

where u is as defined in (1). The first order conditions for consumption and labor are (highlighted in red are the differences with the decentralized equilibrium)

$$
\begin{aligned}
C_t: \;& C_t^{-1} = \lambda_t + 2\lambda_{e,t} e^c C_t \\
L_t: \;& L_t^{\eta} = \lambda_t - 2\lambda_{e,t} e^l \left(1 - M_t\right)^2 L_t \\
M_t: \;& \lambda_t \chi_t M_t = \frac{\beta V_{\bar{M},t+1}}{1 - D_t - \kappa I_t} + 2\lambda_{e,t} e^l \left(1 - M_t\right) L_t^2.
\end{aligned}
$$

The marginal utilities of the planner with respect to exposure are twice as high as those of the private sector because of the contagion externalities: private agents only care about how their behavior affect their own infection risk. They do not care about how their behavior affects the infection risk of others. This is also reflected in the following envelope condition (again, changes relative to the equilibrium are highlighted in red) with respect to the number of infected people:

$$
\begin{aligned}
V_{I,t} = \kappa \frac{L_t^{1+\eta}}{1+\eta} - \kappa u_\kappa - \kappa \lambda_t \left(L_t - \chi_t M_t^2\right) + \lambda_{e,t} \kappa e^l \left(1 - M_t\right)^2 L_t^2 - \left(1 - \rho\right) \lambda_{I,t} \\
- \gamma e_t S_t \left(\lambda_{I,t} - \lambda_{S,t}\right) - \left(\delta_t \kappa + \delta_t' \kappa^2 I_t\right) \left(\lambda_{D,t} - \lambda_{I,t}\right),
\end{aligned}
$$

where δ_t' denotes the derivative of the fatality rate with respect to the sick population. Let us now consider the planner's incentives to mitigate and contrast them with the private incentives studied in section 3.3.

4.1 Mitigation Incentives

The planner's incentives to avoid infection today depend on $V_{S,t+1} - V_{I,t+1}$. Under the same simplifying assumptions as before, $V_{D,t}$ is approximately constant (and the same as that of private agents):

$$
V_D \approx -\frac{u_d}{1-\beta},
$$

while the values of being infected and remaining susceptible are

$$
\begin{aligned}
V_{I,t} &\approx \sum_{s=0}^{\infty} \beta^s \left(\prod_{\tau=0}^{s-1} \left(1 - \rho + \gamma e_{t+\tau} S_{t+\tau} - \delta\kappa\right)\right) \left(\kappa u_\kappa + \delta\kappa \frac{\beta}{1-\beta} u_d\right) \\
V_{S,t} &= \sum_{s=1}^{\infty} \beta^s \left(1 - \gamma e_{t+s-1} I_{t+s-1}\right)^{s-1} \gamma e_{t+s-1} I_{t+s-1} V_{I,t+s}.
\end{aligned}
$$

The expression for $V_{S,t}$ shows that the planner also suffers from the fatalism effect: risk of future infection, captured by the $\gamma e_{t+s-1} I_{t+s-1}$term, reduces the value of remaining susceptible today. But, there is an additional effect which arises because of the $\gamma e_{t+\tau} S_{t+\tau}$ term in the expression for $V_{I,t}$. This implies that the planner's value of infection $V_{I,t}$ becomes even more negative when she becomes aware of the disease. Intuitively, the possibility of an infected individual spreading the disease to susceptible individuals lowers the effective recovery rate from the planner's point of view to $\rho - \gamma e_t S_t$ is instead of ρ. Thus, for the planner, both $V_{I,t}$ and $V_{S,t}$ become more negative when the disease arrives. The net effect, which drives her incentives to mitigate, depend on the relative strength of the two forces. Early on, the risk of an infected agent spreading the disease to others is quite high (since S_t is high) while the fatalism effect is relatively muted (since it takes some time for I_{t+s} to rise). Therefore, $V_{S,t} - V_{I,t}$ rises upon impact, i.e. the planner finds it optimal to increase mitigation as soon as she becomes aware of the disease's arrival.

Finally, while we abstracted from congestion effects in this discussion for simplicity, re-introducing them creates additional incentives for the the planner to mitigate. To see why, note that with congestion effects, the planner's value of infection is given by (the terms that change relative to the case without congestion are highlighted in red):

$$V_{I,t} = \sum_{s=0}^{\infty} \beta^s \left(\prod_{\tau=0}^{s-1} (1 - \rho + \gamma e_{t+\tau} S_{t+\tau} - \delta_{t+\tau} \kappa) \right) \left(\kappa u_\kappa + \delta_{t+s} \kappa \frac{\beta}{1-\beta} u_d + \delta'_{t+s} \kappa^2 I_{t+s} \frac{\beta}{1-\beta} u_d \right).$$

Thus, the planner dislikes infection even more in the presence of congestion effects. This externality introduces another wedge between the private and social incentives to mitigate. This tension helps explain episodes like the Florida spring break controversy. In March 2020, as the arrival of the pandemic became broadly known in the US, many people chose to enjoy their spring break, arguing that if they were going to catch the virus, now would be as good a time as later, while public officials worried about the spread of the disease and hospitals being overwhelmed.

5 Calibration

Before detailing our calibration strategy, we note that considerable uncertainty about key parameters remains even now. For an early discussion of the challenges, see Atkeson (2020a). We return

to this issue later in the paper. We calibrate our model at a weekly frequency.

Contagion The SIR block of the model is parameterized as follows. The recovery parameter is set to $\rho = 0.35$ per week following Atkeson (2020b). This value implies that the average duration for which an infected agent is contagious is about 20 days. The fraction of infected people who fall sick is $\kappa = 0.15$. For the exposure function, we normalize $\bar{e} + e^c + e^l = 1$ and set $e^c = e^l = \frac{1}{4}$, broadly consistent with the estimates in Ferguson (2020). These parameters imply that total exposure $e = 1$ at the pre-pandemic levels of consumption and labor (the calibration of production and utility parameters will be described later). The parameter γ is then chosen to target the basic reproduction number (i.e. the average number of people infected by a single infected individual) of $\mathcal{R} = 2.0$ consistent with the estimate of Salje et al. (2020), yielding an estimated value of $\gamma = 0.7$. Finally, to parameterize the fatality rate and the congestion effects, we adopt the following functional form for the probability of death δ_t :

$$\delta_t = \bar{\delta} + \exp(\phi I_t) - 1,$$

where the parameter ϕ indexes the strength of the congestion externality. We set $\bar{\delta}$ and ϕ to match two targets for the infection mortality rate:[3] a baseline value (the fraction of infected people who die even in the absence of congestion i.e. with $\delta_t = \bar{\delta}$) of 0.25%, which triples when 20% of the population requires medical attention (i.e. the fatality rate when $\kappa I = 0.15 \times 0.2 = 0.03$ is 0.75%). This procedure yields $\bar{\delta} = 0.006$ and $\phi = 0.4$. We examine the robustness of our results to these assumptions about fatality rates later in the paper.

Preferences and technology The utility parameter u_d is set to a value of 2.5 which corresponds to a large non-monetary cost associated with loss of life. We pick a value in the lower end of the range of existing estimates to be consistent with the age profile of COVID-19 fatalities.[4] The flow

[3] The infection fatality rate is given by $\frac{\delta_t \kappa}{\delta_t \kappa + \rho}$.

[4] For example, Greenstone and Nigam (2020) use an estimated value of a statistical life of $11.5 million (in 2020 dollars) for the average population. Assuming a rate of return of 5%, this translates into an annual flow value of $575,000, roughly 10 times per capita GDP, which would imply a u_d of 10. However, COVID-19 deaths are not uniform in the population so using an average VSL may not be the right strategy. According to the CDC, only 0.2 percent of COVID-19 victims were younger than 25, while the median age was above 75 and the average around 75. We therefore make an adjustment based on relative life expectancy, which is 12 years at age 75 and 42 at the median age of 38. This suggests a factor of 0.25 between the average victim and the average agent in our model, which leads to a value of u_d around 2.5.

disutility from sickness u_κ is set to a value of 0.5. The discount factor is set to an annual value of 0.95 or equivalently, a weekly $\beta = (0.95)^{\frac{1}{52}}$.

Next, we calibrate the working-from-home technology, which involves picking values for two parameters – $\bar{\chi}$ and Δ_χ. For the former, we use estimates of the effect of the restrictions imposed by many countries in February and March 2020. A back-of-the-envelope calculation suggests that a policy of maximal mitigation (e.g. requiring almost the entire labor force to work from home $m \approx 1$) with no prior experience ($\overline{m} \approx 0$) causes GDP to fall by 25% below its normal level. Since this initial productivity loss is exactly equal to $\frac{\bar{\chi}}{2}$, we set $\bar{\chi} = 0.5$. Finally, for the long-run parameter, Δ_χ, we rely on Dingel and Neiman (2020), who estimate that roughly one-third of the jobs in the US can be done from home. Guided by this estimate, we set $\Delta_\chi = 0.34$. We also assume that accumulated learning depreciates very slowly, i.e. $\rho_m = 0.99$, which implies that the stock of knowledge evolves according to $\bar{m}_{t+1} = 0.99\bar{m}_t + m_t$.

Finally, we assume that a vaccine arrives a year after the onset of the disease but is only slowly rolled out so it takes 6 months for the entire population to be inoculated. This would likely have been at the optimistic end of the forecasts made by experts in the Spring of 2020 but nevertheless seems like a natural starting point for our analysis.[5]

6 Quantitative Results

Our benchmark exercise assumes an initial infection rate of $I_0 = 1\%$ for expositional purposes (it makes the figures easier to read in the early periods), but it is important to keep in mind that this is a relatively large shock or equivalently, a situation where agents and policy-makers become aware of the pandemic quite late. As part of our robustness analysis, we will also report simulations with different initial infection shocks to capture the possibility of an earlier detection (which is the relevant case for many countries/regions).

Private Response We start with the decentralized solution. Figure 1 shows the behavior of the contagion and macro variables in the decentralized equilibrium under three different assumptions

[5] We assume that during the rollout, the vaccinated are treated the same as everyone else. Needless to say, there are gains to be had by conditioning policies on vaccination status, e.g. by introducing so-called vaccine passports. But, as of the writing of this draft, no country has introduced any concrete steps in this direction, providing some support for our assumption. Moreover, quantitatively, this is unlikely to have a big effect – in part because across all our simulations, the vaccine arrives relatively late.

Figure 1: Decentralized Equilibrium

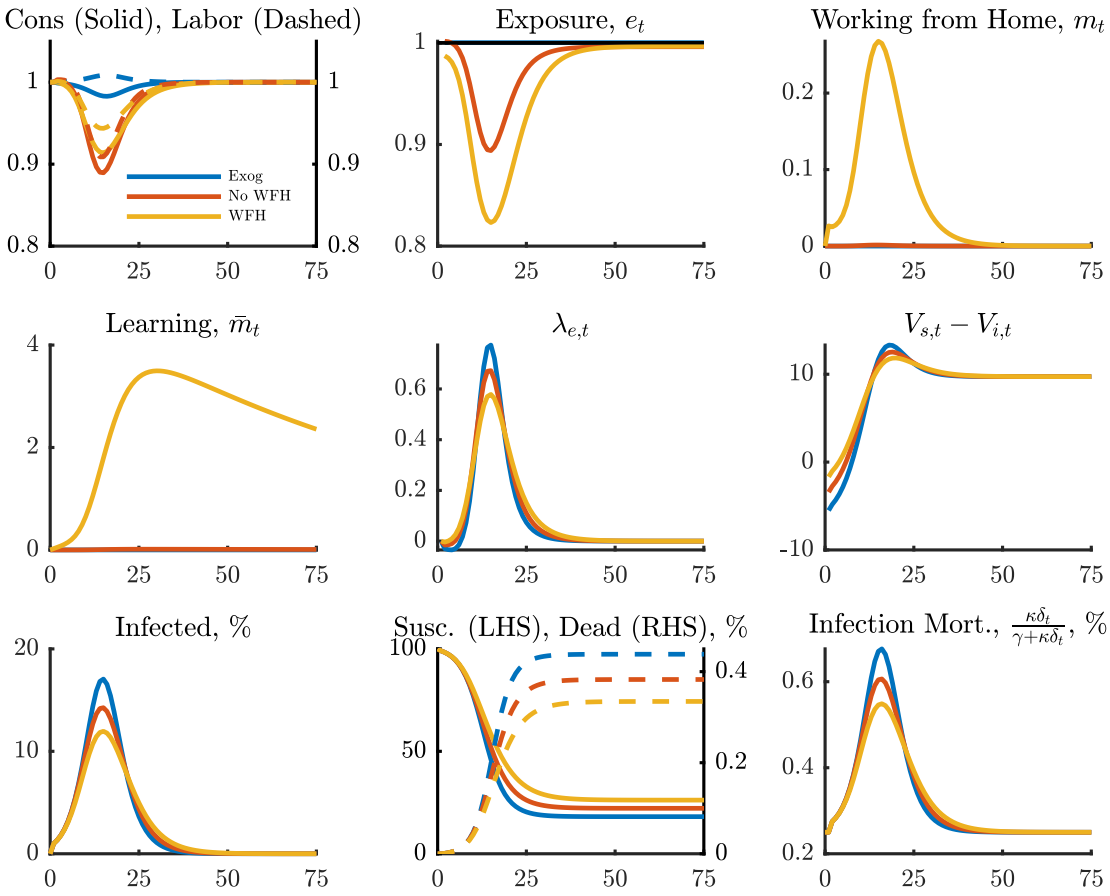

about exposure and mitigation strategies. The solid blue line shows a situation where infection rates are exogenous, i.e. do not vary with the level of economic activity. Since infection is assumed to be exogenous, agents do not engage in mitigation, i.e., they ignore the pandemic. In fact, labor input rises (the dashed line, top left panel in Figure 1), while per-capita consumption falls by about 2% (the solid line), as able-bodied workers work harder to compensate for the workers who are sick. This is clearly not a realistic assumption, but it serves as a useful benchmark for the worst case scenario. In this scenario, almost the entire population is eventually infected (about 82%) and 0.44% of the population succumbs to the virus (bottom, middle panel in Figure 1). The case mortality rate peaks at 0.7% roughly 15 weeks after the initial infection when about 2.6% ($\kappa \times I$ of the peak infection rate of 17%) of the population is sick and the healthcare system is overwhelmed.

The red line describes the case where exposure is endogenous (i.e. varies with consumption and labor) but there is no work-from-home (WFH) technology, i.e, the only way for the household to reduce exposure is to cut back on consumption and labor supply. As we would expect, this leads

to a sharp reduction in economic activity (top, left panel in Figure 1) – almost 11% at the trough. Importantly, the reduction is gradual, tracking the overall infection rate (consumption and labor hit their lows at 17 weeks). Intuitively, when the fraction of infected people is low (as is the case in the early stages), a reduction in exposure has a small effect on future infection risk, relative to the resulting fall in consumption. And since each household does not internalize the effect it has on the future infection rate, it has little incentive to indulge in costly mitigation early on. This dynamic is reflected in the hump-shaped pattern in λ_e (the middle panel in Figure 1). As we will see, the planner's incentives change much more strongly at the beginning. The mitigation behavior does lower the cumulative infection and death rates (relative to the exogenous infection case) by about 5% and 0.6% respectively.

Finally, the yellow line shows the effect of access to the WFH technology. This allows the household to reduce exposure without sacrificing consumption – now, the peak loss in consumption is 8.7%, even as the exposure falls by more (0.82 compared to 0.9, top middle panel in Figure 1). Mitigation (e.g. fraction of time spent working from home) in the top, right panel in Figure 1 is hump-shaped, peaking at almost 30% at the same time as the fraction infected. This additional flexibility also lowers cumulative fatalities to 0.3%. However, the timing of mitigation strategies is mostly unchanged – households in the decentralized economy do not find it optimal to front-load their mitigation efforts.

Optimal Response We now turn to the planner's solution, depicted in Figure 2. As before, the blue, red and yellow lines show the cases of exogenous infection, mitigation without WFH and mitigation with WFH, respectively. As the yellow and red curves in Figure 2 show, the planner finds it optimal to "flatten the curve" more dramatically than agents in equilibrium. The peak infection rates are well below the decentralized equilibrium levels (7% versus 12%), leading to a lower peak fatality rate (0.4% versus .55%) as well as cumulative deaths (0.23%, compared to just over 0.3% in the decentralized equilibrium with WFH). To achieve this, the planner has to cut exposure by almost 30%. Of course, this pushes the economy into a deeper recession with consumption falling by 27% even with WFH (top left panel in Figure 2). The planner's response also displays a hump-shaped pattern, rising with the infection rate, but she does step on the brakes sooner (immediately upon learning of the disease) compared to private agents.

Figure 2: Planner Solution: Contagion Dynamics

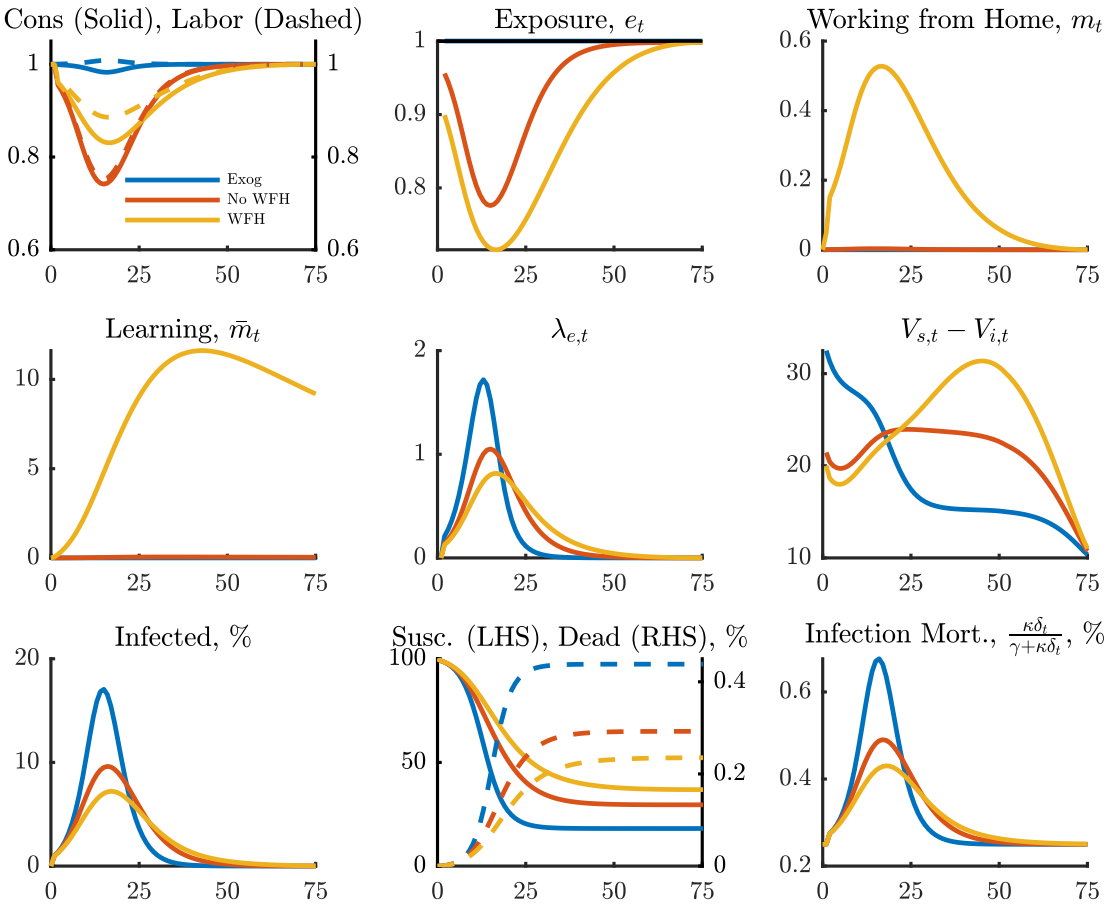

The availability of the WFH technology ameliorates the economic impact of the planner's suppression strategy, but does not significantly alter the contagion dynamics. Intuitively, fatalities are so costly that the planner aggressively suppresses the infection even in the absence of the WFH option: access to WFH simply allows the planner to achieve the same exposure outcomes at a lower cost. Notice also that the planner's incentives to use the WFH technology are much stronger than that of private agents in a decentralized equilibrium: partly because her shadow value of exposure is higher but also because she attaches a greater value to the future benefits of accumulated knowledge. As a result, m rises to as high as 0.5 relatively quickly (compared to 0.3 in the decentralized equilibrium).

How do these patterns look relative to observed outcomes? Take the experience of the state of New York. Between March and September 2020, NY's GDP fell by about 10.5% (relative to a pre-Covid trend) and cumulative excessive deaths were about 0.21% of its population. In the

Figure 3: Fatalism and Perverse Incentives

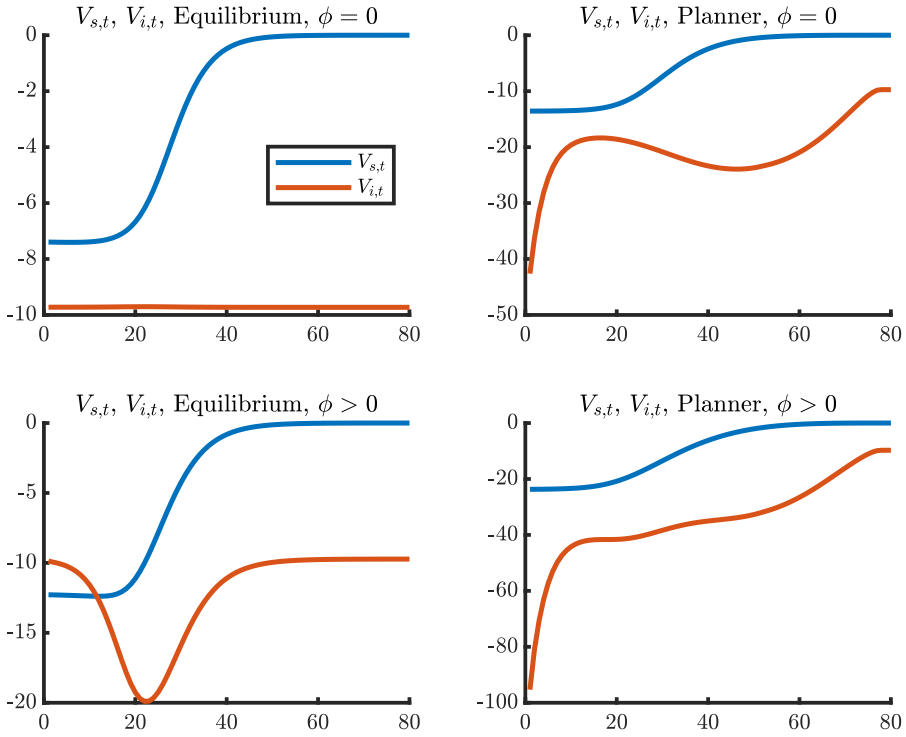

planner's solution above, the average decline in GDP is about 12% (relative to pre-pandemic) over the first 26 weeks from the time disease was detected with a death toll of 0.17% of the population.

Private versus Public Incentives Figure 3 illustrates the fatalism effect. The top graphs assume a constant risk of death δ. On the left we see the shrinking private incentives for safety early on as $V_{s,t} - V_{i,t}$ decreases. On the right, we see that $V_{s,t} - V_{i,t}$ increases for the planner. The lower graphs illustrate another incentive problem that arises when δ is time-varying. If agents anticipate congestion in the future and if they think they are likely to become infected, they might prefer to increase their risk of infection today because it is better to be sick when δ is still relatively low. Not only does $V_{s,t} - V_{i,t}$ shrink, its sign can even flip, as we see in the bottom left panel. For the planner, by contrast, the risk of a higher δ increases the incentives to mitigate. We conclude that the misalignment of private incentives is larger during early stages of the epidemic and is amplified by congestion externalities.

Early versus Late Detection Next, we analyze the effect of the planner becoming aware of the disease earlier. Recall that, in the baseline, the planner became aware of the disease when $I_0 = 1\%$.

Now, we suppose instead the planner becomes aware of the disease much earlier, specifically at $I_0 = 0.01\%$. Figure 4 shows her optimal response in this case. The changes relative to the $I_0 = 1\%$ case are relatively small – the extent of mitigation, work-from-home and the final death count are all quite similar across these cases (of course, as we would expect, the peaks occur slightly later with a smaller initial infection). These results suggest a modest value to detecting the disease at an earlier stage.

This exercise also offers an useful way to think about differences in observed outcomes across regions. For example, consider two regions which differ in the infection rate at the time of detection of the epidemic. One region (say, the state of New York) started its response only after the disease had already infected 1% of the population while another region (say, California) was able to start mitigation at a small initial infection rate of 0.01%. The model predicts significant difference in health outcomes after 10 months – the fraction of the population dead after 40 weeks in the model is 0.22% in the late detection region and 0.13% in the early detection region. These line up reasonably well with the data – cumulative excess deaths in New York between March 2020 and January 2021 was about 0.26% while the corresponding number for California was 0.14%.

This also shows how a large country like the United States with many regions can experience second waves, due to a compositional effect – just as the disease wanes in one region, it picks up steam in another.

Fatality Rates As we discussed earlier, there is still little agreement in the literature on the mortality of Covid-19, with Atkeson (2020a) suggesting that the range of plausible values could be as wide as 0.1% to 1%. To explore the effect of this uncertainty, we repeat our analysis of the planner's problem with a mortality rate of 1% or four times our baseline value and at the top of the range suggested by Atkeson (2020a). The results are presented in Figure 5. As expected, the overall number of fatalities are much higher, as is the economic cost. The fraction of the population dying from the disease rises to about 0.6% over the course of the pandemic. The profile of the planner's solution shifts towards substantially more mitigation throughout: she still finds it optimal to begin mitigation almost immediately and at a higher level and maintains tight mitigation throughout. As a result, the drop in consumption reaches about 15% immediately and bottoms out around 30% six months after the initial infection shock. The infection curve is substantially flattened, with peak

infections cut almost in half.

Congestion Externality Next, to isolate the role of the congestion externality, we repeat our analysis of the planner's solution with the parameter ϕ set to 0. The results, shown in Figure 6, display similar patterns as Figure 2 but with a much less severe contraction. Intuitively, a healthcare system with sufficient slack capacity allows the planner to achieve similar outcomes in terms of fatalities with modestly higher infection rates or equivalently, with less mitigation (top, right panel in Figure 6). Accordingly, the recession is not as deep or persistent than in the baseline.

Altruistic Households Finally, we consider the possibility that households partly internalize their effects on the aggregate outcome. Formally, we assume that households incorporate externalities with a weight τ while making their consumption, labor and mitigation decisions. The *laissez-faire* equilibrium and the planner's optimum are obtained as special cases by setting $\tau = 0$ and $\tau = 1$ respectively. If $\tau = 0.33$, cumulative deaths are reduced to 0.3% (a little lower than the 0.33% under $\tau = 0$). If τ is assumed to be 0.5, i.e. households place equal weight on private and social incentives, the cumulative death rate falls slightly to 0.29% (roughly half of the gap between the *laissez-faire* equilibrium and the planner's optimum). These results suggest that for private decisions to be close to that of the planner requires a very large degree of altruism.

Parameter Uncertainty As we briefly alluded to earlier, there was (and in some respects, continues to be) much uncertainty about the structural parameters of the disease. Here, we use our model to speak to the dilemma faced by policy-makers who have to make decisions with imperfect knowledge of key primitives. Atkeson (2020a) points out that, when one does not know the initial number of active cases, it is difficult "to distinguish whether the disease is deadly (1% fatality rate) or milder (0.1% fatality rate)." We illustrate this in Figure 7 where we show how very different combinations of primitives can have similar implications for the number of deaths, the variable that is arguably the best measured. The graph shows the evolution of the disease in the absence of any mitigation for two cases. The first case has a baseline reproduction number $\mathcal{R} = 3$ and an infection fatality rate of 0.5%, while the other has a lower reproduction number $\mathcal{R} = 2$ but a higher infection fatality rate of 1%. With an initial shock of $i_0 = 1\%$, over the first two months of the spread, the paths of the number of dead are almost identical, as shown in the first panel of

Figure 4: Planner Solution: Two States with 1% and 0.01% Initial Infection Shocks

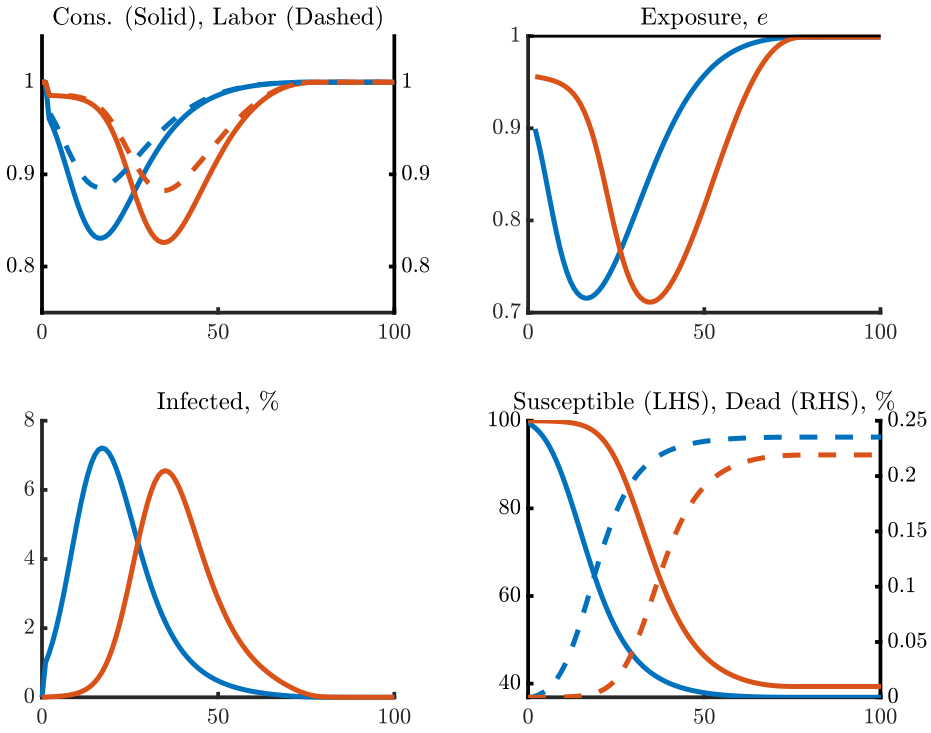

Figure 5: Planner Solution: Aggregates with Increased δ_t

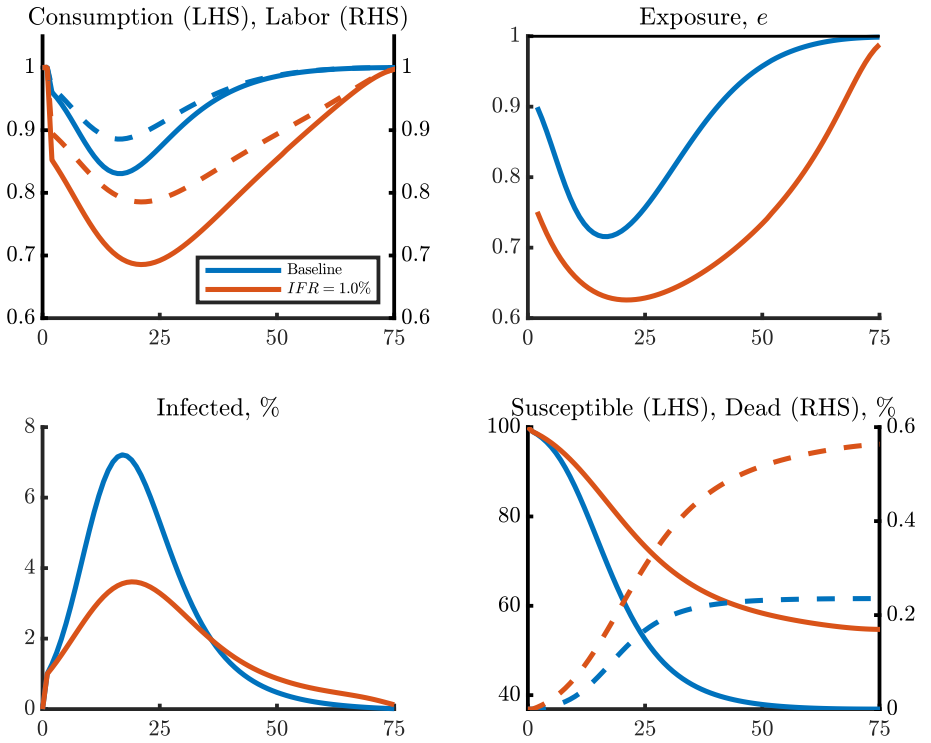

Figure 6: Planner Solution: Aggregates with $\phi = 0$

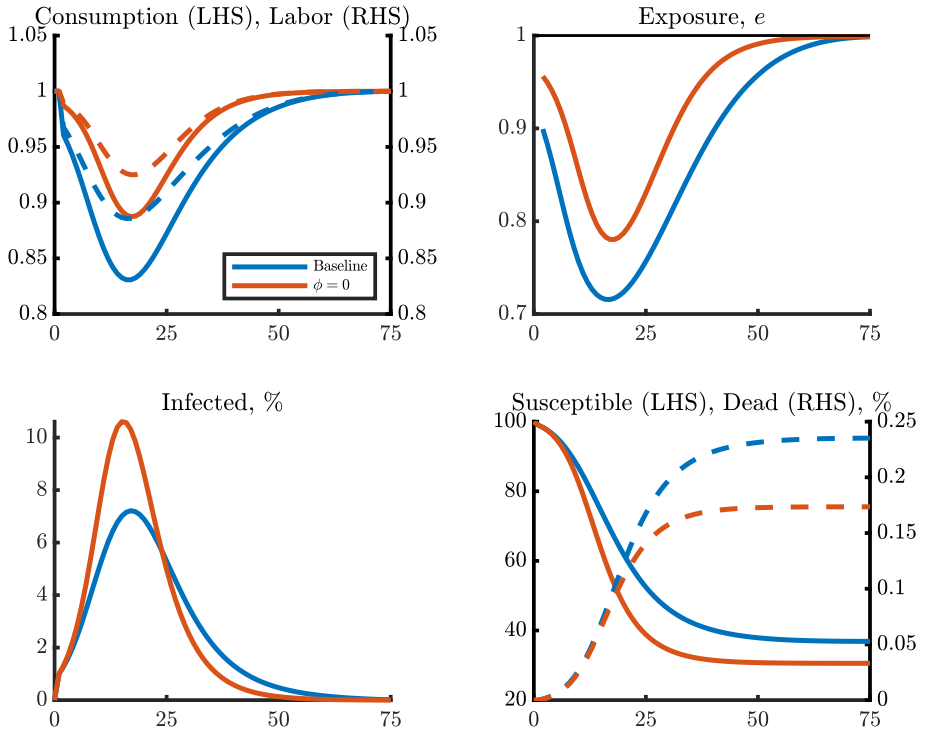

the figure. Without accurate measures of other epidemiological variables, such as the number of newly infected or the fraction of cases recovered, it would be nearly impossible to distinguish the two diseases in the short-term. Over the longer-term, however, the two diseases have very different implications for the number of dead, as shown in the second panel.

To explore the role of this uncertainty, we look at the optimal policy of a planner under the two cases (starting from an initial value of $i_0 = 0.1\%$). The planner's choices for labor, consumption and exposure are shown in Figure 8. Interestingly, during the first few weeks, the planner's choices are quite similar under both cases – she cuts exposure by almost 10% immediately. The differences between the two cases become noticeable only after 8-10 weeks – the planner continues to ramp up mitigation aggressively for the more contagious (albeit less fatal) case while the less contagious version induces a more measured but persistent increase. This pattern suggests the following strategy for a planner faced with large uncertainty about the fatality rate: aggressively mitigate the spread of the disease for the first few weeks while waiting for more data. Assuming there is a substantial reduction in uncertainty within the first 10 weeks after the outbreak, this strategy will allow the planner to implement the optimal response, despite the initial uncertainty about a key

Figure 7: Percentage of Population Dead for Two Diseases and Time Horizons

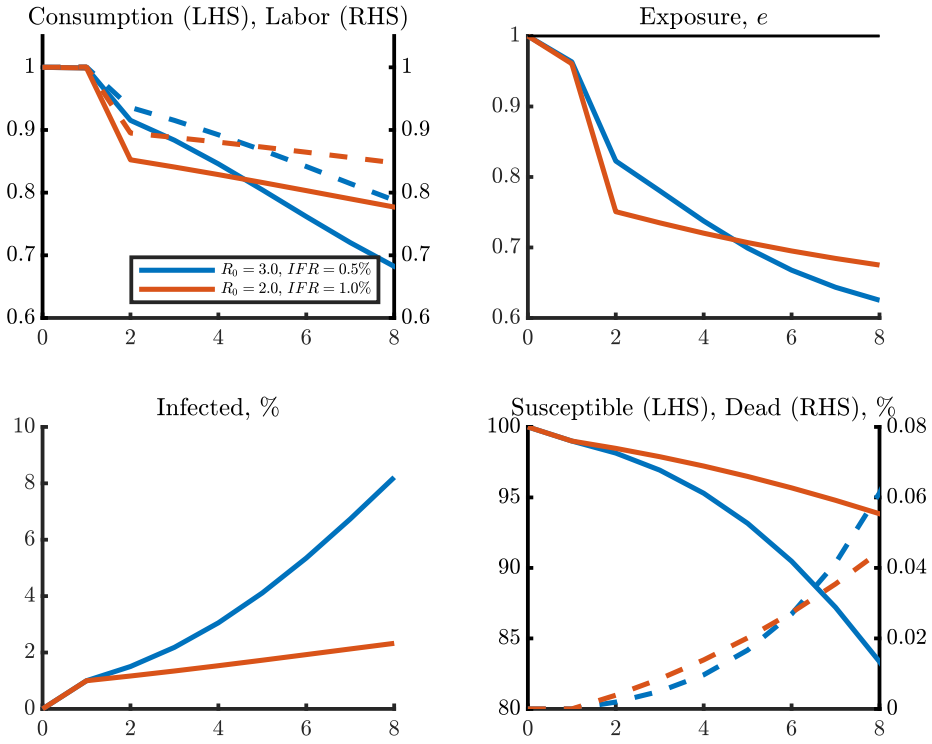

parameter.

Time-varying Mortality and Exposure Our baseline model held key parameters fixed throughout the pandemic. This allowed us to highlight the dynamic incentives – both private and social – for mitigation. Here, we explore the implications of time variation, specifically in fatality and exposure rates.

In our first experiment, we study the effect of a declining fatality rate, capturing, e.g. improvement in treatment of the disease (either because of the arrival of new drugs/cures or due to learning-by-doing). Specifically, we contrast the planner's optimal solution when the fatality rate falls by half over the course of first 6 months to her strategy under a constant (high) fatality rate. The former is modeled using an adjusted fatality rate of $\hat{\delta}_t = \left(1 - \frac{t}{26}\frac{1}{2}\right)\delta_t$ for $t \leq 26$ and $\hat{\delta}_t = \frac{\delta_t}{2}$ otherwise. The results are plotted in the orange lines in Figure 9. The blue lines show the optimal response when the fatality rate is the unadjusted δ_t. The comparison between the two lines shows an interesting pattern — a planner who anticipates a declining mortality rate mitigates

Figure 8: Percentage of Population Dead for Two Diseases and Time Horizons

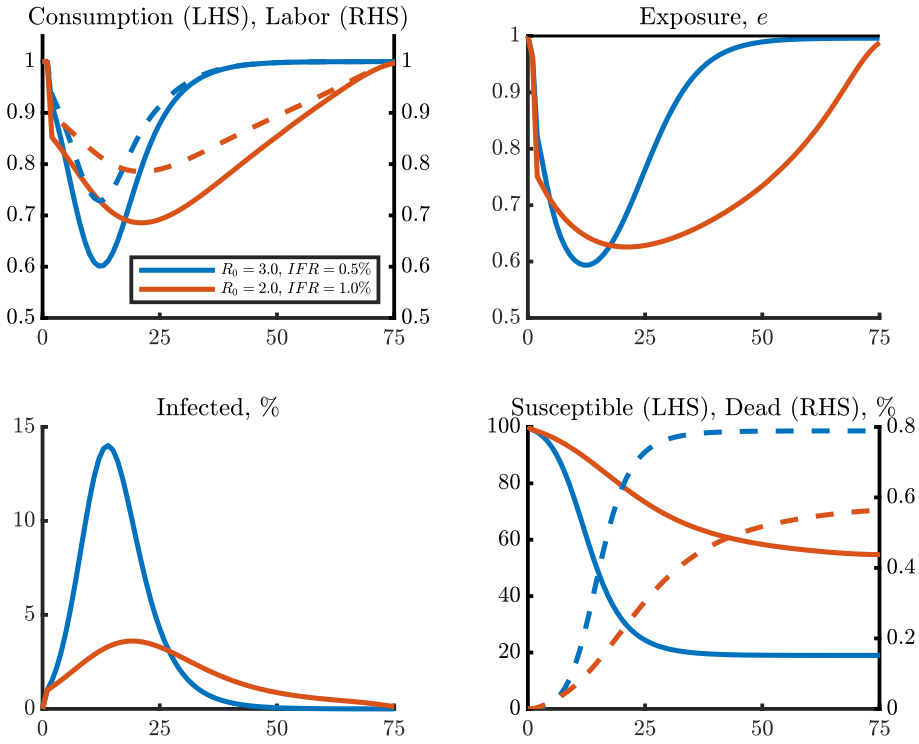

more (less) aggressively early (later) on in the disease's spread. Intuitively, she finds it optimal to delay infections, moving them from the high to the low mortality phase.

In the second experiment, we let the baseline exposure $\bar{e}$ vary over time. Recall that this parameter is meant to capture risk of infection unrelated to economic activity, e.g. through social events or other interactions. This is related, among other things, to weather and other seasonal factors (such as holidays). To capture this type of time variation, we solve for the socially optimal path under the assumption that $\bar{e}$ doubles from its baseline value at week 24, before slowly returning to its original value over the following 6 months. Figure 10 shows the key variables in this case (the orange lines) compared to the baseline in blue. This creates a mini second wave of infections, but quantitatively, the effects are somewhat modest with about 0.03% additional deaths in the long run. Interestingly, anticipation of $\bar{e}$ rising in the future causes the planner to slightly scale back her initial mitigation during the early stages.

Pandemic Fatigue Finally, we consider the effects of pandemic fatigue. Formally, we add a direct utility cost associated with mitigation

Figure 9: Planner Solution: Time-Varying Fatality

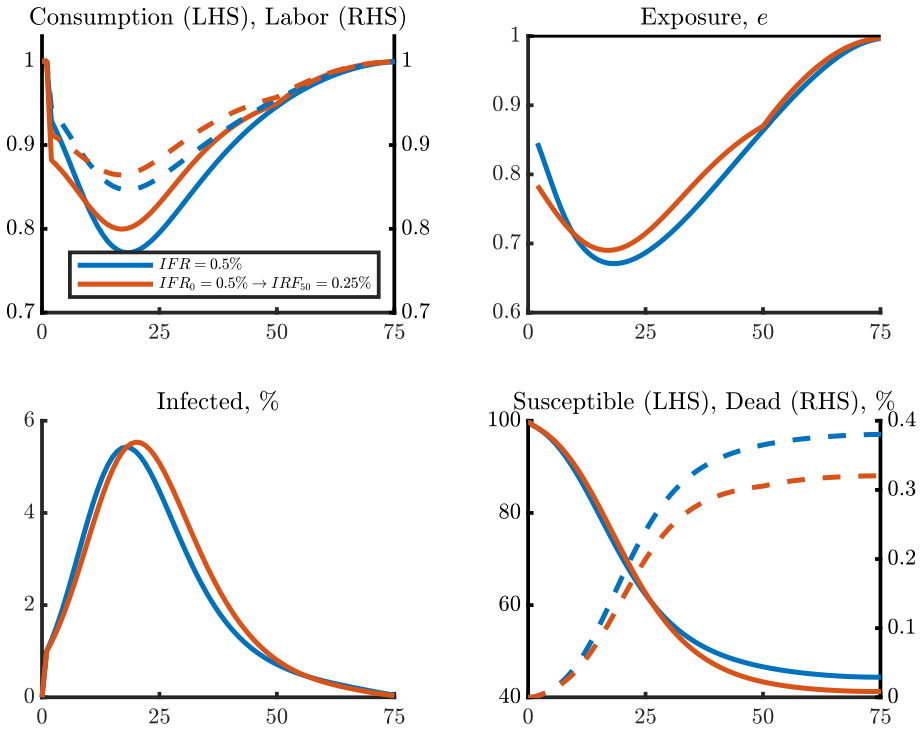

Figure 10: Planner Solution: Time-Varying Exogenous Exposure

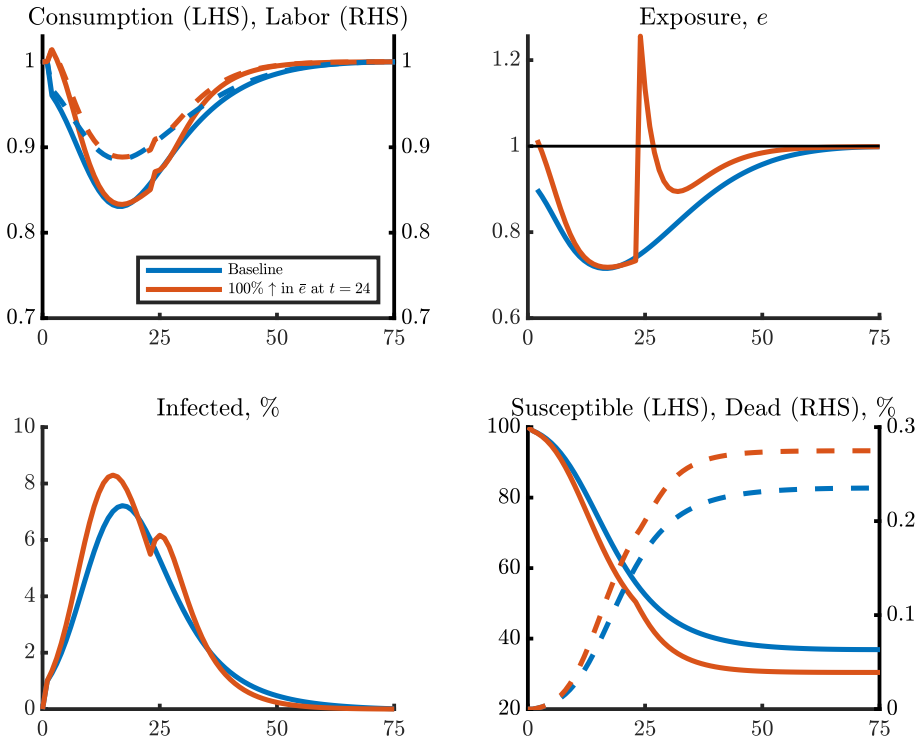

$$u\left(C_t, L_t; I_t, D_t\right) = \left(1 - D_t\right)\log\left(C_t\right) - \left(1 - D_t - \kappa I_t\right)\frac{L_t^{1+\eta}}{1+\eta} - \frac{\omega_1}{2}F_t^{\omega_2}M_t^2 - u_\kappa \kappa I_t - u_d D_t$$

$$F_{t+1} = \rho_f F_t + M_t$$

where F_t denotes fatigue or accumulated past mitigation (with a 'depreciation' rate of $1 - \rho_f$) and ω_1, ω_2 are parameters. Note that the disutility of mitigation is increasing in fatigue, which introduces another dynamic consideration – avoiding infection today makes it costlier to undertake mitigation in future periods. The planner's solution in the presence of fatigue is shown in Figure 11, along with the baseline, no-fatigue version.[6] As one would expect, the presence of fatigue lowers overall mitigation, though the effects on overall health and economic outcomes are quite modest (cumulative deaths in the planner's solution rise only by about 0.05% relative to the baseline). These results suggest that our baseline findings are robust to the presence of this type of fatigue.

7 Sectoral Heterogeneity

We extend our baseline to allow for multiple sectors that differ in their epidemiological parameters and ability to work from home. This will allow us to compare the model's predictions to detailed micro data on sector-level health and economic outcomes. We will focus on the planner's solution. Formally, consumption is a composite of J different goods,

$$C_t = \left(\sum_{j=1}^{J} \xi_j C_{jt}^{\frac{\theta-1}{\theta}}\right)^{\frac{\theta}{\theta-1}}$$

where each good is produced according to

$$Y_{jt} = \hat{L}_{jt} = \left(1 - D_t - \kappa I_t\right)\left(L_{jt} - \frac{\chi_{jt}}{2}M_{jt}^2\right)$$

[6] We use the following values for the fatigue parameters: $\omega_1 = 0.5, \omega_2 = 0.5, \rho_f = 0.99$.

Figure 11: Planner Solution: Social Distancing Fatigue v No Fatigue

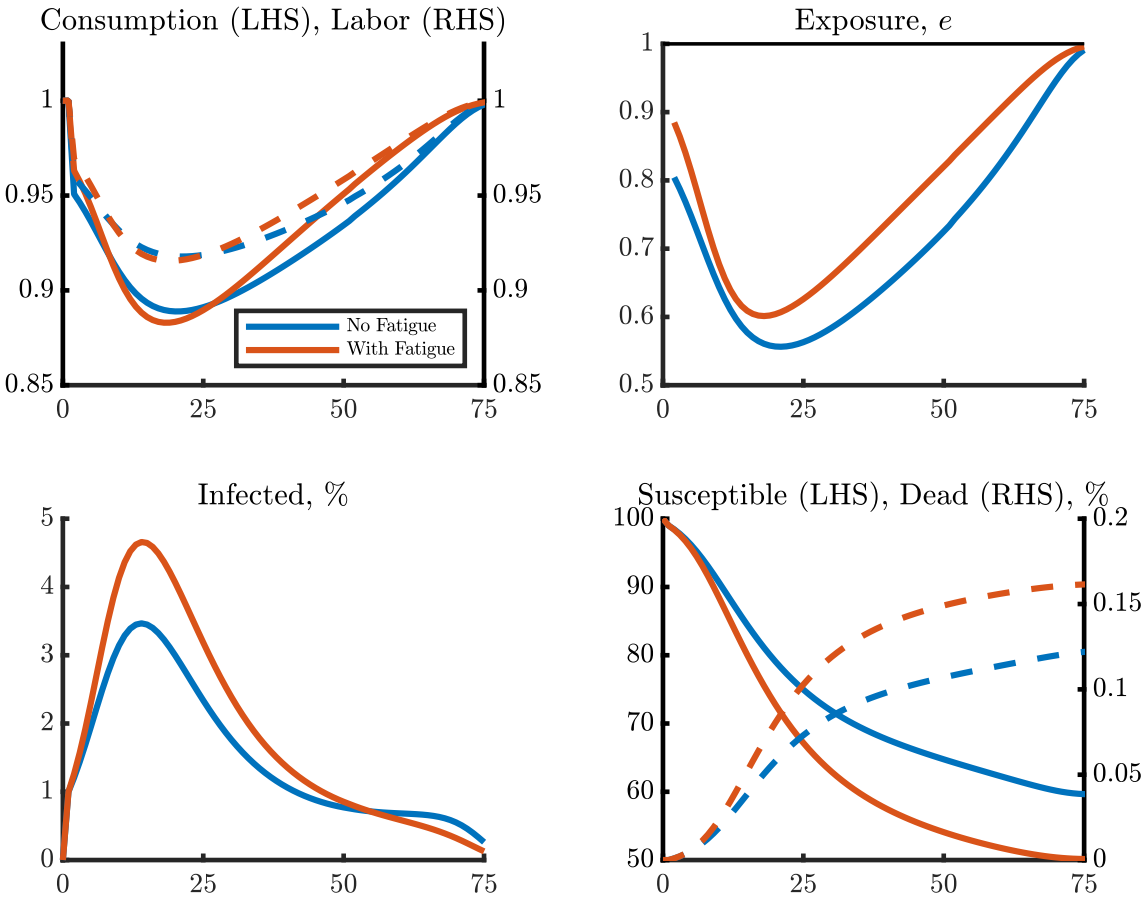

with sector-specific mitigation cost and learning-by-doing processes given by

$$\chi_{jt} = \bar{\chi}_j \left(1 - \Delta_{\chi j} \left(1 - \exp\left(-\overline{M}_{jt}\right)\right)\right)$$
$$\overline{M}_{jt+1} = \rho_M \overline{M}_{jt} + M_{jt}$$

Total exposure is the sum of consumption and production exposures across the three sectors

$$e_t = \bar{e} + (1 - D_t) \sum_j e_j^c C_{jt}^2 + (1 - D_t - \kappa I_t) \sum_j e_j^l \left(1 - M_{jt}\right)^2 L_{jt}^2$$

Thus, the sectors differ in the exposure risk – captured by the parameters $\left(e_j^c, e_j^l\right)$ – and in the productivity losses associated with mitigation, i.e. in $(\bar{\chi}_j, \Delta_{\chi j})$.

We calibrate a version with 3 sectors of High, Medium and Low infection risks. The calibration strategy, along with values for the exposure and mitigation parameters, is in Appendix C. The results – specifically, economic and health outcomes 26 weeks after the onset of the pandemic – are summarized in the red bars in Figure 12. The red bars in first panel shows the relative share of infections, defined as $Share_{j,26} = \frac{\sum_{t=1}^{26} e_j^l \gamma S_t I_t (1-D_t-\kappa I_t)(1-M_{jt})^2 L_{jt}^2}{\sum_j \sum_{t=1}^{26} e_j^l \gamma S_t I_t (1-D_t-\kappa I_t)(1-M_{jt})^2 L_{jt}^2}$. The remaining two panels show the average drop in sectoral output over the same period.

The empirical analogues (the blue bars in the figure) are constructed using detailed data from the state of Washington. We first group industries into our High, Medium and Low sectors using the estimated share of jobs that can be done from home in Dingel and Neiman (2020). We then compute the cumulative infection shares and GDP changes for each group. [7]They show that the optimal responses in the model correspond quite closely with the observed outcomes. For example, in the data, the High risk sectors accounted for almost 65% of total infections and suffered a GDP loss of about 8%, compared to 64% and 10% respectively in the model. At the other extreme, the optimal decline in the output of the low risk sectors is about 1%. In the data, those sectors actually experienced a small increase relative to pre-pandemic levels. This increase was driven entirely by

[7]The indutry-wise infection shares are taken from a report titled "COVID-19 Confirmed Cases by Industry Sector" published in November 2020 by the Washington State Department of Health and Washington State Department of Labor and Industries. It is available at https://www.doh.wa.gov/Portals/1/Documents/1600/coronavirus/IndustrySectorReport.pdf. The GDP changes are the percentage changes in real GDP during Q2 and Q3 2020 (relative to Q4 2019) and are computed using the National Income and Product Accounts published by the Bureau of Economic Analysis.

Figure 12: Planner Solution: Multi-Sector Model Versus Data

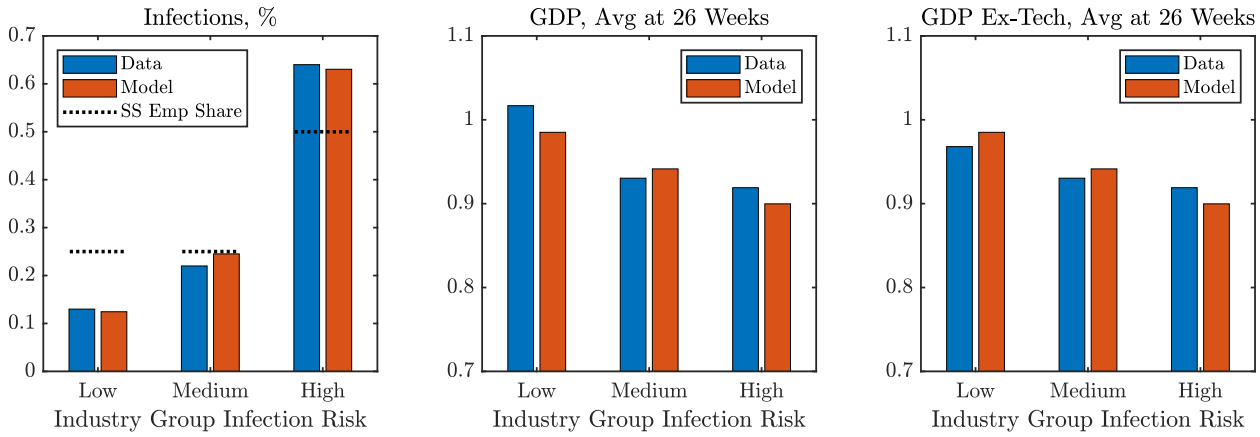

a large boom in the information technology sector: as the third panel shows, the Low risk sector excluding tech experienced a modest decline in GDP during Q2-Q3 of 2020.

8 Conclusions

We propose an extension of the neoclassical model to include contagion dynamics to study and quantify the trade-offs of policies that can mitigate the Covid-19 pandemic. Our model reveals two key insights. Firstly, relative to the incentives of private agents, a planner's incentives to mitigate the spread of the disease are more front-loaded. Secondly, in our calibrated model, the possibility of mitigating the spread of the disease by working from home leads to quantitatively meaningful reductions in the spread of a disease and the economic costs involved.

Our modeling framework was kept simple to more clearly demonstrate the economic forces involved. Nonetheless, it does a good job at predicting the overall economic and epidemiological outcomes observed in the US. An extended version of the model with heterogeneous sectors, which differ in their exposure risk as well as the ability to work from home, also does fairly well at matching the patterns of cross-sectional output and infection incidence.

There are many dimensions along which the model could be enriched to provide sharper quantitative estimates as well as answers to other policy-relevant questions. One interesting direction is to explore asset pricing implications, in particular ask whether the mitigation and learning mechanisms emphasized here can help explain some of the dramatic swings in stock markets during the early stages of the pandemic (see for example, Gormsen and Koijen, 2020, for a careful description

of the asset market evidence during this period). This would not only require adding elements necessary for reasonable asset pricing patterns (such as recursive preferences), but also explicitly incorporate uncertainty and/or learning about epidemiological and mitigation parameters.

Our focus on a simple representative household formulation also abstracts from imperfections in risk-sharing. Understanding how mitigation strategies and dynamics interact with these imperfections in a calibrated version with realistic heterogeneity is another important and interesting avenue for future work. Finally, we have also abstracted from testing and the possibility of more targeted mitigation strategies, yet another dimension where more work needs to be done.

References

Alvarez, Fernando, David Argente, and Francesco Lippi, "A Simple Planning Problem for COVID-19 Lockdown," March 2020. Working Paper.

Atkeson, Andrew, "How Deadly is COVID-19? Understanding the Difficulties with Estimation," March 2020. NBER Working Paper No. 26867.

_ , "What Will Be the Economic Impact of COVID-19 in the US? Rough Estimates of Disease Scenarios," March 2020. NBER Working Paper No. 26867.

Baker, Scott R., R.A. Farrokhnia, Steffen Meyer, Michaela Pagel, and Constantine Yannelis, "How Does Household Spending Respond to an Epidemic? Consumption During the 2020 COVID-19 Pandemic," *University of Chicago, Working Paper*, 2020.

Barro, Robert J, Jose Ursua, and Joanna Weng, "The coronavirus and the Great Influenza epidemic: Lessons from the "Spanish Flu" for the coronavirus' potential effects on mortality and economic activity," March 2020. AEI Economics Working Paper 2020-02.

Berger, David, Kyle Herkenhoff, and Simon Mongey, "An SEIR Infectious Disease Model with Testing and Conditional Quarantine," March 2020. Working Paper.

Correia, Sergio, Stephan Luck, and Emil Verner, "Pandemics Depress the Economy, Public Health Interventions Do Not: Evidence from the 1918 Flu," March 2020. Working Paper.

Diekmann, Odo and J. Heesterbeek, *Mathematical Epidemiology of Infectious Diseases: Model Building, Analysis and Interpretation*, John Wiley, 2000.

Dingel, Jonathan and Brent Neiman, "How Many Jobs Can be Done at Home?," March 2020. Working Paper.

Eichenbaum, Martin, Sergio Rebelo, and Mathias Trabandt, "The Macroeconomics of Epidemics," March 2020. Working Paper NWU.

Ferguson, Neil, "Impact of non-pharmaceutical interventions (NPIs) to reduce COVID- 19 mortality and healthcare demand," March 2020. Imperial College Report.

Gormsen, Niels Joachim and Ralph SJ Koijen, "Coronavirus: Impact on stock prices and growth expectations," *The Review of Asset Pricing Studies*, 2020, *10* (4), 574–597.

Greenstone, Michael and Vishan Nigam, "Does Social Distancing Matter?," *University of Chicago, Becker Friedman Institute for Economics Working Paper*, 2020, (2020-26).

Harko, Tiberiu, Francisco Lobo, and M. K. Mak, "Exact analytical solutions of the Susceptible-Infected-Recovered (SIR) epidemic model and of the SIR model with equal death and birth rates," *Applied Mathematics and Computation*, 2014, (236), 184–194.

Lucas, Robert E. Jr. and Nancy L. Stokey, "Money and Interest in a Cash-in-Advance Economy," *Econometrica,*, 1987, *55* (3), 491–513.

Salje, Henrik, Cécile Tran Kiem, Noémie Lefrancq, Noémie Courtejoie, and Paolo Bosetti et al., "Estimating the burden of SARS-CoV-2 in France," 2020. Institut Pasteur.

Appendix

A Decentralized Equilibrium

The Lagrangian of the household is:

$$
\begin{aligned}
V_t = & \, u\left(c_t, l_t; i_t, d_t\right) + \beta V_{t+1} + \lambda_t \left(\hat{l}_t + b_t - \left(1 - d_t\right) c_t - \frac{b_{t+1}}{1 + r_t}\right) \\
& + \lambda_{e,t} \left(e_t - \bar{e} - \left(1 - d_t\right) e^c c_t C_t - \left(1 - d_t - \kappa i_t\right) e^l \left(1 - m_t\right) l_t \left(1 - M_t\right) L_t\right) \\
& + \lambda_{i,t} \left(i_{t+1} - \gamma e_t \frac{I_t}{N} s_t - \left(1 - \rho\right) i_t + \delta_t \kappa i_t\right) \\
& + \lambda_{s,t} \left(s_{t+1} - s_t + \gamma e_t \frac{I_t}{N} s_t\right) \\
& + \lambda_{d,t} \left(d_{t+1} - d_t - \delta_t \kappa i_t\right)
\end{aligned}
$$

The first order conditions for consumption and labor are then

$$
\begin{aligned}
c_t: \;\; & c_t^{-1} = \lambda_t + \lambda_{e,t} e^c C_t \\
l_t: \;\; & l_t^{\eta} = \lambda_t - \lambda_{e,t} e^l \left(1 - m_t\right) \left(1 - M_t\right) L_t \\
m_t: \;\; & \lambda_t \chi_t m_t = \frac{\beta V_{\bar{m},t+1}}{1 - d_t - \kappa i_t} + \lambda_{e,t} e^l l_t \left(1 - M_t\right) L_t
\end{aligned}
$$

The remaining first order conditions are

$$
\begin{aligned}
e_t : \lambda_{e,t} &= \left(\lambda_{i,t} - \lambda_{s,t}\right) \gamma \frac{I_t}{N} s_t \\
i_{t+1} : \lambda_{i,t} &= -\beta V_{i,t+1} \\
s_{t+1} : \lambda_{s,t} &= -\beta V_{s,t+1} \\
d_{t+1} : \lambda_{d,t} &= -\beta V_{d,t+1}
\end{aligned}
$$

The envelope conditions are

$$V_{i,t} = \kappa \frac{l_t^{1+\eta}}{1+\eta} - \kappa u_\kappa - \kappa \lambda_t \left(l_t - \frac{\chi_t m_t^2}{2} \right) + \lambda_{e,t} \kappa e^l \left(1 - m_t\right) l_t \left(1 - M_t\right) L_t - \left(1 - \rho\right) \lambda_{i,t} + \delta_t \kappa \left(\lambda_{i,t} - \lambda_{d,t}\right)$$

$$V_{s,t} = \left(\lambda_{s,t} - \lambda_{i,t}\right) \gamma e_t \frac{I_t}{N} - \lambda_{s,t}$$

$$V_{d,t} = \frac{l_t^{1+\eta}}{1+\eta} - \log\left(c_t\right) - u_d - \lambda_t \left(l_t - \chi_t m_t^2 - c_t \right) + \lambda_{e,t} \left(e^c c_t C_t + e^l \left(1 - m_t\right) l_t \left(1 - M_t\right) L_t \right) - \lambda_{d,t}$$

$$V_{\overline{m},t} = \beta V_{\overline{m},t+1} + \lambda_t \left(1 - d_t - \kappa i_t\right) \frac{\bar{\chi}}{2} m_t^2 \Delta_\chi \exp\left(-\overline{m}_t\right)$$

These first-order and envelope conditions, the equations governing SIR dynamics, exposure, and mortality rate, and the market clearing conditions, characterize the equilibrium.

B Planner's Problem

We normalize $N = 1$ for simplicity. The planner solves

$$\max U = \sum_{t=0}^{\infty} \beta^t u\left(C_t, L_t; I_t, D_t\right)$$

subject to

$$u\left(C_t, L_t; I_t, D_t\right) = \left(1 - D_t\right) \log\left(C_t\right) - \left(1 - D_t - \kappa I_t\right) \frac{L_t^{1+\eta}}{1+\eta} - u_\kappa \kappa I_t - u_d D_t$$

and

$$\left(1 - D_t\right) C_t = \left(1 - D_t - \kappa I_t\right) \left(L_t - \frac{\chi\left(\bar{M}_t\right)}{2} \left(M_t\right)^2 \right)$$

and the SIR equations

$$S_{t+1} = S_t - \gamma e_t I_t S_t$$

$$I_{t+1} = \gamma e_t I_t S_t + \left(1 - \rho\right) I_t - \delta\left(\kappa I_t\right) \kappa I_t$$

$$D_{t+1} = D_t + \delta\left(\kappa I_t\right) \kappa i_t$$

$$R_{t+1} = R_t + \rho I_t$$

The Lagrangian is

$$\begin{aligned}
V_t\left(I_t, S_t, D_t, \bar{M}_t\right) =& u\left(C_t, L_t; I_t, D_t\right) + \beta V_{t+1} + \lambda_t\left(\left(1 - D_t - \kappa I_t\right)\left(L_t - \chi\left(\bar{M}_t\right)\left(M_t\right)^2\right) - \left(1 - D_t\right) C_t\right) \\
&+ \lambda_{e,t}\left(e_t - \bar{e} - \left(1 - D_t\right) e^c C_t^2 - \left(1 - D_t - \kappa I_t\right) e^l \left(1 - M_t\right)^2 L_t^2\right) \\
&+ \lambda_{i,t}\left(I_{t+1} - \gamma e_t I_t S_t - \left(1 - \rho\right) I_t + \delta\left(\kappa I_t\right) \kappa I_t\right) \\
&+ \lambda_{s,t}\left(S_{t+1} - S_t + \gamma e_t I_t S_t\right) \\
&+ \lambda_{d,t}\left(D_{t+1} - D_t - \delta\left(\kappa I_t\right) \kappa I_t\right)
\end{aligned}$$

The first order conditions for consumption and labor are then (highlighted in red the difference with the decentralized equilibrium)

$$\begin{aligned}
C_t: \;& C_t^{-1} = \lambda_t + 2\lambda_{e,t} e^c C_t \\
L_t: \;& L_t^{\eta} = \lambda_t - 2\lambda_{e,t} e^l \left(1 - M_t\right)^2 L_t \\
M_t: \;& \lambda_t \chi_t M_t = \frac{\beta V_{\bar{M},t+1}}{1 - D_t - \kappa I_t} + 2\lambda_{e,t} e^l \left(1 - M_t\right) L_t^2
\end{aligned}$$

The remaining first order conditions are the same as those of the private sector

$$\begin{aligned}
e_t &: \lambda_{e,t} = \left(\lambda_{i,t} - \lambda_{s,t}\right) \gamma I_t s_t \\
I_{t+1} &: \lambda_{i,t} = -\beta V_{I,t+1} \\
S_{t+1} &: \lambda_{s,t} = -\beta V_{S,t+1} \\
D_{t+1} &: \lambda_{d,t} = -\beta V_{D,t+1}
\end{aligned}$$

The envelope conditions are

$$V_{I,t} = \kappa \frac{L_t^{1+\eta}}{1+\eta} - \kappa u_\kappa - \kappa \lambda_t \left(L_t - \frac{\chi_t}{2} M_t^2 \right) + \lambda_{e,t} \kappa e^l \left(1 - M_t\right)^2 L_t^2 - (1-\rho)\, \lambda_{i,t}$$
$$-\gamma e_t S_t \lambda_{i,t} - \left(\delta_t \kappa + \delta_t' \kappa^2 I_t \right) \left(\lambda_{d,t} - \lambda_{i,t} \right)$$
$$V_{S,t} = -\lambda_{s,t} - \gamma e_t I_t \left(\lambda_{i,t} - \lambda_{s,t} \right)$$
$$V_{D,t} = \frac{L_t^{1+\eta}}{1+\eta} - \log\left(C_t\right) - u_d - \lambda_t \left(L_t - \frac{\chi_t}{2} \left(M_t\right)^2 - C_t \right) + \lambda_{e,t} \left(e^c C_t^2 + e^l \left(1 - M_t\right)^2 L_t^2 \right) - \lambda_{D,t}$$
$$V_{\bar{M},t} = \beta V_{\bar{M},t+1} + \lambda_t \left(1 - D_t - \kappa I_t\right) \frac{\bar{\chi}}{2} \Delta_\chi e^{\bar{M}_t} \left(M_t\right)^2$$

C Multisector Model: Calibration

We first order the (NAICS 2-digit) industries by the share of jobs that can be done from home, as estimated by Dingel and Neiman (2020) and reported under the column marked WFH Index in Table 2 below.[8] We then group them into 3 sectors – a High infection-risk sector (accounting for a cumulative 50% of pre-Covid employment), a Medium infection-risk sector (accounting for the next 25% of pre-Covid employment), and a Low infection-risk sector (accounting for the remaining 25% of pre-Covid employment). We will denote these sectors with subscripts $j = 1, 2, 3$ respectively.

There are four parameters that differ across sectors: e_j^l the exposure through labor, e_j^c the exposure through consumption, and $\bar{\chi}_j$ and $\Delta_{\chi j}$ which govern productivity losses associated with working-from-home mitigation. We set the sector-specific parameters of the medium infection-risk sector to their values in our baseline, one-sector model. We then scale the parameters of the High and Low infection-risk sectors by the relative WFH indices. These average WFH indices for the High, Medium and Low infection-risk sectors are 0.76, 0.45 and 0.19 respectively, so the corresponding factors are 1.69, 1 and 0.42. The calibrated parameters are given in Table 1.

[8] Specifically, we use the wage-weighted measures reported in Table 3 of their paper. The employment shares reported in Table 2 are taken from a report titled "COVID-19 Confirmed Cases by Industry Sector" published in November 2020 by the Washington State Department of Health and Washington State Department of Labor and Industries. It is available at https://www.doh.wa.gov/Portals/1/Documents/1600/coronavirus/IndustrySectorReport.pdf.

Table 1: Calibrated Parameters, Multisector Model

		High	Medium	Low
e_j^l	Labor Exposure	0.42	0.25	0.11
e_j^c	Consumption Exposure	0.42	0.25	0.11
$\bar{\chi}_j$	Mitigation Cost	0.84	0.5	0.21
$\Delta_{\chi j}$	Max Mitigation	0.57	0.34	0.14

Table 2: Industries Used in Multisector Analysis

		WFH Index	Emp. Share	Group
72	Accommodation and Food Services	0.07	0.09	High
11	Agriculture, Forestry, Fishing and Hunting	0.13	0.03	High
44-45	Retail Trade	0.22	0.12	High
23	Construction	0.22	0.06	High
62	Health Care and Social Assistance	0.24	0.13	High
48-49	Transportation and Warehousing	0.25	0.04	High
31-33	Manufacturing	0.36	0.09	Medium
71	Arts, Entertainment, and Recreation	0.36	0.02	Medium
21	Mining, Quarrying, and Oil and Gas Extraction	0.37	0.005	Medium
22	Utilities	0.41	0.01	Medium
81	Other Services (except Public Administration)	0.43	0.03	Medium
56	Admin / Support, Waste Mgmt, Remediation	0.43	0.05	Medium
99	Federal, State, and Local Government	0.47	0.04	Medium
53	Real Estate and Rental and Leasing	0.54	0.02	Low
42	Wholesale Trade	0.67	0.04	Low
61	Educational Services	0.71	0.09	Low
51	Information	0.80	0.04	Low
52	Finance and Insurance	0.85	0.03	Low
55	Management of Companies and Enterprises	0.86	0.02	Low
54	Professional, Scientific, and Technical Services	0.86	0.06	Low

The Emp Share column reports the percentage of employment in Washington state and is taken from the report titled "COVID-19 Confirmed Cases by Industry Sector" (publication number 421-002, dated November 10, 2020) published by the Washington State Department of Health and Department of Labor and Industries. It is available here.

D Properties of Contagion Dynamics

D.1 Definitions

We start with the most basic concept in epidemiology, the basic reproduction number, which we denote by $\mathcal{R}$ because the usual notation "R_not" is terribly confusing. $\mathcal{R}$ is the expected number of cases directly generated by one case when everyone else is susceptible. The most basic model is to assume that when someone is infected there are three stages

1. a latency period T_1 when the individual is not yet infectious
2. infectious period $T_2 - T_1$
3. recovered period after T_2 when the individual is not infectious anymore

If the contact rate (exposure) is e and the probability of infection conditional on contact is γ, the expected number of secondary cases per primary case in a fully susceptible population is therefore

$$\mathcal{R} = \gamma e \left(T_2 - T_1 \right)$$

In our notations, e is the number of people that one individual meets per unit of time and γ is the probability of transmitting the disease conditional on a meeting between one infectious and one susceptible agent.

D.2 SIR Model

The SIR model builds on this idea. We define the length of one period so that $T_1 = 1$. If someone is infected in period t, then she will start spreading the disease in period $t+1$. Let I_t be the number of infected individuals and S_t the number of susceptible individuals at the beginning of time t in a population of size N. Each infected agent meets e people. We assume that the meetings are random and that the population is always evenly mixed, therefore the probability of meeting a susceptible person is S/N. The number of meetings between infected and susceptible agents is therefore eIS/N and the total number of new infections is $\gamma e I_t \frac{S_t}{N}$. In our macro model e is an endogenous variable but we take it as a constant for now. We assume that recovery follows a Poisson process with

intensity ρ. The infection equation is then

$$I_{t+1} = \gamma e I_t \frac{S_t}{N} + (1-\rho)\, I_t \tag{12}$$

Consider a population of size N (large) of initially susceptible individuals ($S_0 = N$). If one individual is infected, the total number of secondary infections from that individual is

$$\mathcal{R} = \sum_{\tau=0}^{\infty} \gamma e\, (1-\rho)^{\tau} = \frac{\gamma e}{\rho} \tag{13}$$

Note that $\mathcal{R}$ is a number, not a rate per unit of time. The model has a steady state at $I = 0$ and $S = 1$ but it is unstable in the sense that if one individual gets infected the system converges to a different steady state. In general we can write

$$\frac{I_{t+1}}{I_t} = 1 + \gamma e \frac{S_t}{N} - \rho$$

When $S/N \approx 1$, the number infected people evolves exponentially as $\frac{I_{t+1}}{I_t} \approx 1 + \gamma e - \rho$. If $R_0 < 1$ then a small infection disappears exponentially. If $R_0 > 1$ then there is an epidemic where I initially grows over time. The growth continues as long as $\gamma e \frac{S_t}{N} > \rho$. Eventually the number of susceptible people decreases and growth slows down or reverses, depending on how we close the model.

There are two ways to close the model. The simpler one, called the SIS model, assumes that recovered agents ρI go back to the pool of susceptible agents. This is the model used to study the common cold. In that case $N = S_t + I_t$ and the equation becomes

$$I_{t+1} = \gamma e I_t \frac{N - I_t}{N} + (1-\rho)\, I_t$$

and the steady state infection rate is $\frac{I}{N} = \max\left(0; 1 - \frac{\rho}{\gamma e}\right)$.

The other way is to introduce a population of recovered agents R who are not susceptible anymore. This model – called SIR – is used for flu epidemics, among others. In the simple model,

R is an absorbing state. The system becomes

$$S_{t+1} - S_t = -\gamma e I_t \frac{S_t}{N} \tag{14}$$

$$R_{t+1} - R_t = \rho I_t \tag{15}$$

and of course $N = S_t + I_t + R_t$. Note that S is (weakly) decreasing and R is (weakly) increasing, therefore their limits exist. Since $N = S_t + I_t + R_t$ so does the limit of I. For R and S to be constant it must be that I tends to zero. Therefore

$$\lim_{t\to\infty} I_t = 0$$

That is the first simple property of the solution. Second, since S is decreasing, I must be (at most) single-peaked. If I_0 is small and $R_o > 1$ then I_t must grow, reach a maximum, and then decrease towards zero. This is the typical shape of the curves found in the literature. Harko et al. (2014) provide an analytical solution to the differential equations (in continuous time).

Let us now study the long run behavior of S and R. Combining equations (14) and (15) we get

$$R_{t+1} - R_t = -N \frac{\rho}{\gamma e} \frac{S_{t+1} - S_t}{S_t}$$

This equation is simpler to write in continuous time

$$\frac{\dot{S}}{S} = -\frac{\gamma e}{\rho} \frac{\dot{R}}{N}$$

and to integrate the solution:

$$\log\left(\frac{S_t}{S_0}\right) = -\frac{\gamma e}{\rho}\left(\frac{R_t - R_0}{N}\right)$$

This equation holds along any transition path without exogenous shocks. In the limit, since $S_\infty + R_\infty = 1$ we have the transcendental equation

$$\log\left(\frac{S_\infty}{S_0}\right) = -\frac{\gamma e}{\rho}\left(\frac{1 - S_\infty - R_0}{N}\right)$$

The long run steady state (S_∞, R_∞) depends on the initial conditions as well at the basic repro-

duction number $\mathcal{R}$. We can summarize our discussion in the following Lemma.

Lemma. *The SIR model is fully characterized by* $\mathcal{R} = \frac{\gamma e}{\rho}$ *and the initial conditions* (S_0, R_0). *If* $\mathcal{R} < 1$, *infections die out without epidemic. If* $\mathcal{R} > 1$, *a small infection* I_0 *creates an epidemic:* I_t *rises, reaches a maximum in finite time before declining towards zero:* $I_\infty = 0$. *The long run limits* S_∞ *and* R_∞ *exist and satisfy* $S_\infty + R_\infty = 1$ *and* $\log\left(\frac{S_\infty}{S_0}\right) = -\mathcal{R}\left(\frac{1-S_\infty-R_0}{N}\right)$.

The complete model takes into account that some individuals will die from the disease. We assume that a fraction κ of infected agents become (severely) sick and a fraction δ of the sick patients die. Hence we have another absorbing state, D. The system of equation of the $SIRD$ model becomes

$$\begin{aligned} I_{t+1} &= \gamma I_t \frac{S_t}{N} + (1 - \rho - \delta\kappa) I_t \\ S_{t+1} &= S_t - \gamma I_t \frac{S_t}{N} \\ R_{t+1} &= R_t + \rho I_t \\ D_{t+1} &= D_t + \delta\kappa I_t \end{aligned}$$

The number of sick people is κI_t and determines the pressure on the health care system. From the perspective of the epidemic we could aggregate D and R into one absorbing state: $\tilde{R} = D + R$ such that $\tilde{R}_{t+1} = \tilde{R}_t + (\rho + \delta\kappa) I_t$. The long run solution is

$$\log\left(\frac{S_\infty}{S_0}\right) = -\frac{\gamma e}{\rho + \delta\kappa}\left(\frac{1 - S_\infty - \tilde{R}_0}{N}\right)$$

and $\tilde{R}_\infty = 1 - S_\infty$ while $D_\infty = D_0 + \frac{\delta\kappa}{\delta\kappa+\rho}\left(\tilde{R}_\infty - \tilde{R}_0\right)$. From an economic and social perspective we need to keep track of D and R separately in any case.

D.3 SIR model with exogenous birth and death

The path dependence of the long run steady state is a somewhat artificial consequence of the lack of entry and exit. Suppose that ϵN people are both in state S each period, and also that there is

a constant exogenous death rate ϵ. The system is

$$\begin{aligned} I_{t+1} &= \gamma e I_t \frac{S_t}{N} + (1 - \rho - \epsilon) I_t \\ S_{t+1} &= (1 - \epsilon) S_t - \gamma e I_t \frac{S_t}{N} + \epsilon N \\ R_{t+1} &= (1 - \epsilon) R_t + \rho I_t \end{aligned}$$

Note that population is constant: $S_{t+1} + I_{t+1} + R_{t+1} = N$. Now the steady state requires

$$\begin{aligned} \gamma e \frac{S}{N} I &= I (\epsilon + \rho) \\ \gamma e I \frac{S}{N} &= \epsilon (N - S) \\ \rho I &= \epsilon R \end{aligned}$$

Since $I > 0$ we can easily solve for the unique steady state

$$\begin{aligned} \frac{S}{N} &= \frac{\epsilon + \rho}{\gamma e} \\ \frac{I}{N} &= \epsilon \frac{1 - \frac{\epsilon + \rho}{\gamma e}}{\epsilon + \rho} \\ \frac{R}{N} &= \rho \frac{1 - \frac{\epsilon + \rho}{\gamma e}}{\epsilon + \rho} \end{aligned}$$

And now we can take the limit as $\epsilon \to 0$ to get $\frac{I}{N} = 0$, $\frac{S}{N} = \frac{\rho}{\gamma e} = \mathcal{R}^{-1}$ and $\frac{R}{N} = 1 - \frac{\rho}{\gamma e} = 1 - \mathcal{R}^{-1}$. Adding a small amount of exogenous birth and death would render the long run steady state independent of initial conditions.